THE DESIGN AND DEVELOPMENT OF A NOVEL ROBOTIC EXOSKELETON FOR PATIENTS SUFFERING FROM BRACHIAL PLEXUS INJURY

By

Peter Anderson, Hons. B.Sc.

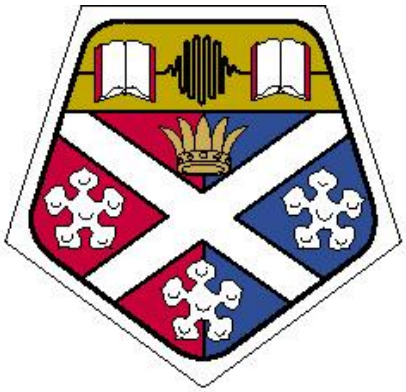

UNIVERSITY OF STRATHCLYDE

A THESIS SUBMITTED IN PARTIAL FULFILLMENT OF THE REQUIREMENTS FOR THE DEGREE OF

MASTER OF SCIENCE IN BIOMEDICAL ENGINEERING

AT

THE UNIVERSITY OF STRATHCLYDE
12/08/2014

SUPERVISOR: Dr Heba Lakany

This thesis is the result of the author's original research. It has been composed by the author and has not been previously submitted for examination which has led to the award of a degree.

I would like to express my gratitude to the staff of the Biomedical Engineering Unit of the University of Strathclyde, namely Dr. Heba Lakany Stephen Murray, and Christine McGonagle of the National Centre of prosthetics and Orthotics. Without their academic and practical expertise I could not have completed this Thesis.

Additionally, special thanks go to Mr. Kevin Quillian and Ms. Amy Anderson for their unwavering support, both personal and academic.

Signed: _____

Dated: _____

CONTENTS

1. TABLE OF CONTENTS Page

TABLE OF CONTENTS [Continued] PAGE

CONTENTS

LIST OF FIGURES AND TABLES

LIST OF FIGURES Page

CONTENTS

LIST OF FIGURES AND TABLES

LIST OF TABLES Page

Abstract

Brachial Plexus injury is a debilitating condition first described in 1779 that affects more than 1 in a 100 adults in the US, and between 0.5-3 per 1000 live births. This condition is severely limiting and can result in varying degrees of hemiparesis in the patient. This condition in adults often arises through vehicular accidents and as such has been rising throughout the 20th century. Since 1779, many rehabilitative techniques have been pioneered – mostly surgical – such as nerve suturing and shoulder arthrodesis to varying degrees of success.

However, as modern technology decreases in size and increases in power, prosthetics and orthotics have come into the fore. Amputation followed by a prosthetic application, though medically sound, is rejected by a large proportion of patients – even with a likelihood of a better prognosis. Orthoses prove to be much less invasive than amputation and therefore is often a preferred option of many patients Though even with many advancements in the field, many modern orthotics are often expensive, cumbersome and require attending physicians to supervise rehabilitation of the patient in a laboratory setting.

This research contains a proposal for a novel orthotic for an adult that is safe, cheap, easy to interface with, and is able to be worn throughout the patients' daily life with maximum assistance and minimal obstruction. The research will be presented first as a background and literature review on current orthotics, followed by a discussion and critical analysis on both the electrical and mechanical components and finally a design proposal.

Due to time constraints, it was not possible to obtain and prototype the components – however, the underlying mechanical and electrical theory and components have been analysed and presented in this research paper.

Chapter 1

Introduction

1-1 Literature Review and Background

Nerves are the base component of the complex nervous system found in almost all multicellular organisms; these nerves form organic pathways which allow the transmission or reception of electrochemical signals by the brain. The transmission or reception of these signals will lead to a specific type of effect dependant on the area of the brain/body part stimulated. There are two types of neurons present in an organism; motor neurons and sensory neurons. Motor neurons transmit electrical signals away from the brain and through the spinal column, which combined are known as the central nervous system, and through the peripheral nervous system in order to stimulate a specific effector cell. The peripheral nervous system is the term used to describe every nerve and ganglia found out-with the CNS and leads to every cell cluster and muscle fibre within the body. The effector cell can therefore be an array of different types of cells with different functions. Upon nervous system stimulation a cell will react according to the cells differentiated function; for example, stimulated Cardiac Myocytes (muscle cells) will depolarize leading to altered gene expression, production of neurotransmitters and ultimately contraction of the tissue – I.e. a heartbeat.

Sensory neurons, in contrast, receive information from the peripheries – information such as touch, heat and sound. Each of these stimuli causes an electrical signal to be sent through the peripheral nervous system into the CNS and finally into the brain - -- where the signal is interpreted. This allows the organism to make an appropriate reaction based on the type of signal and strength of signal. For example, during the event of pain or tissue trauma, Substance P is released by endothelial cells. This substance is a neurotransmitter which is picked up at the point of damage by sensory neurons, causing an electrical signal to be sent to the brain to inform of the location and extent of tissue damage.

The human body has millions upon millions of neuronal cells; there are estimated that there are almost 100 billion neurons found in the brain alone. Although not fully understood, the nervous system is vast, complex and efficient where Information is travelled along these organic pathways at almost 3560m/second; allowing the host organism to interpret and react to the world around it.

Figure 1

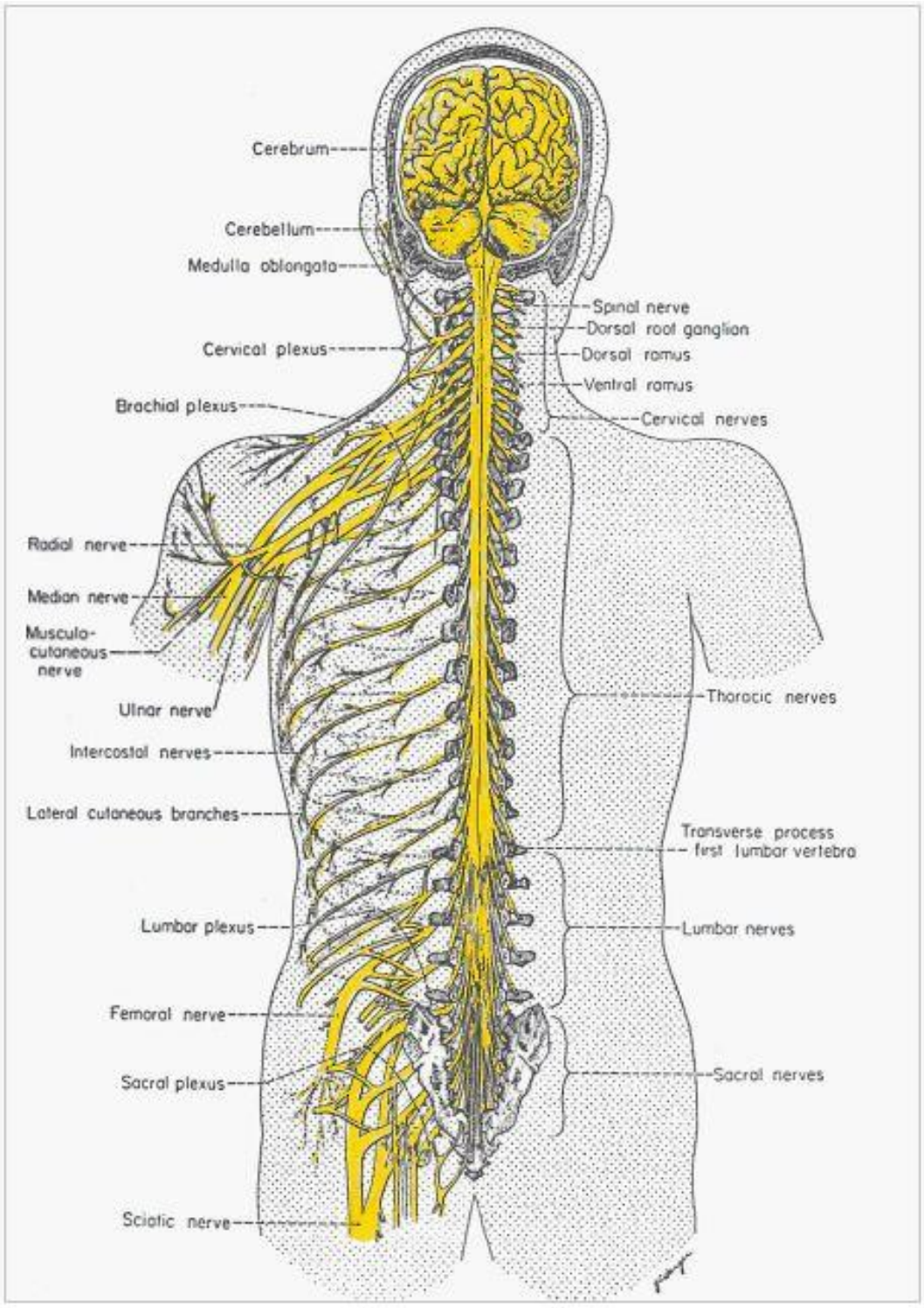

Figure 1 shows the main nerves compromising the nervous system in the upper body and brain. The central nervous system can be clearly seen; from the brain (cerebrum) throughout the spine. The peripheral nervous system is the nerves seen leading away from the spine into other tissues; for example the brachial plexus, which innervates the upper shoulder and arm. SOURCE: Anatomy 9535 J.A Kiernan in the Department of Anatomy and Cell Biology at the University of Western Ontario.

1-1 Brachial Plexus Injury

The brachial plexus is a nerve cluster found in the upper limb of the human body; the roots of which extend from the C5- T1 vertebrae nerve ganglions which are attached to the spinal cord (see figure 2). These nerve fibres run the length of the arm, delivering the brains electrochemical signals towards the brachium (upper arm), the antebrachium (forearm), hand and fingers. The structure of the brachial plexus which can be seen to originate from 5 main vertebrae; each vertebrae containing different nerve branches which stimulate different muscles in the upper limb. Combining this with the data from table one [see appendix], it can be seen that the brachial plexus structure is responsible for the innervation of the full muscular structure of the arm the pectoralis major/minor and back muscles including the latissimus dorsi and teres major muscle groups [see appendix].

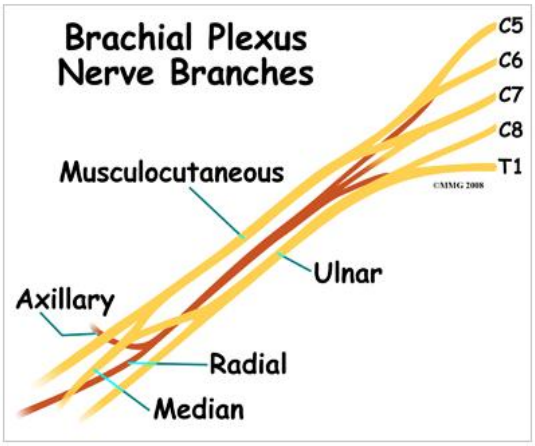

Figure 2 shows the brachial plexus nerve cluster. C5-T1 represents the vertebrae of the spine from which the root extends; the lower 4 cervical vertebrates and the first thoracic vertebrae. It can be seen to be compromised of several nerve fibres which extend down along the entire arm.
SOURCE: Houston Methodist Orthopaedics and Sports Medicine

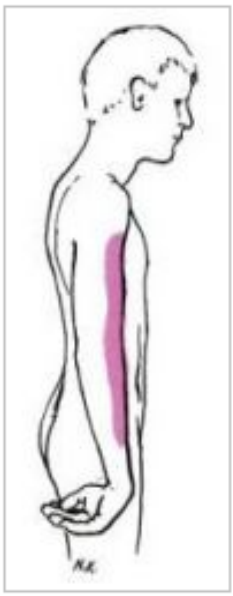

Figure 3 shows a diagrammatic representation of the 'waiters tip', with purple designating the internal rotation.

Specific injury and the consequences of this injury were first observed in 1779 by the British obstetrician, William Smellie, who described a unilateral paralysis suffered by a neonate following a difficult birthing procedure [1]. This paralysis was lifelong affliction; however, the mechanism of injury wasn't fully described until French Neurologist Duchenne noticed the electrical pattern of an upper root injury and proposed that 'Traction during birth' as the root cause – 'pulling' of the head away from the body during birth causing a downward pressure at the shoulder causing nervous damage in the brachial plexus nerve cluster.

The extent of paralysis may vary dependently on how many roots were damaged during trauma; the most common plexus injury is Erb's palsy, or upper brachial injury, was first observed in 1874 and is due to physical injury of the C5 – C6 invertebrae nerve roots. This presented, according to Wilhelm Erb, with weakness in the patients' bicep, forearms, triceps and deltoids. This physically manifests as a 'waiters tip' deformity, in which the arm is adducted and internally rotated at the shoulder. Additionally the wrist is pronated and extended causing the 'tip' [2].

1-2 Types of Brachial Plexus injury

In addition to Erbs' palsy, Augusta Klempke in 1885 first described nerve damage to C8 to T1 vertebras (occasionally also C7) – the lower roots of the brachial plexus. This was associated with tricep, forearm and wrist paralysis; distinguishing it from Erbs' palsy as the patients' control of the bicep and shoulders remained. This can be understood by reading of the table of the appendix, where it states that C8/T1 is directly responsible for the innervation of the Medial Cord (which innervates the antebrachium) and the Radial nerve (triceps innervation).

The second most common Brachial plexus injury is a full injury; in which all nerve roots are avulsed between C5 and T1 – presenting with total motor malfunction and paralysis. This presents in the patients as a flail arm, with little to no sensation and usually full paralysis. This type of injury is also the more prevalent injury seen in adults; most often the cause relating to sports injuries or high speed vehicular accidents, specifically motorcycle accidents where patients are thrown forward off their bike.

Since 1885, many other variations of nerve avulsions have been found; Kerr et al. found at least 29 variants of nerve damage and in another study later found a further 38 variants [7]. Studies later found a key difference in terms of treatment and rehabilitation is whether or not the injury is pre-ganglionic or post-ganglionic. In the PNS, there is an area known as a 'ganglion' which acts as an intermediary between two nerve fibres; the preganglionic nerve and the postganglionic nerve. Preganglionic nerve clusters directly interact with the spine, and generally carry nerve impulses and sensory information to and from the periphery into the spine. Postganglionic nerve clusters directly interact with the effector cell/organ to induce a specific response.

In terms of rehabilitation, preganglionic injuries have the worst prognosis as they are due to complete avulsion of the roots from the vertebrae; surgery may only provide slight, if any, functional restoration. However, postganglionic injuries are associated with disruption of the long nerve fibre, and under the correct therapy may regenerate to almost full use [8].

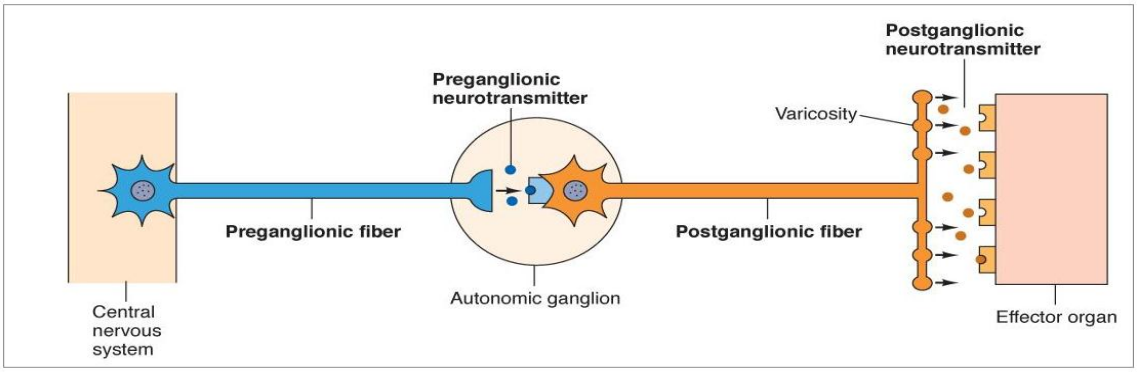

Figure 4 shows pathway from the CNS-> Preganglionic Nerve Fibres -> Ganglion -> Postganglionic fibres which ends with the innervation of the effector muscle/tissue.
SOURCE: Copyright Brooks/Cole – Thomson Learning

1-3 Treatments for Brachial Plexus Injuries

Between 0.2-2 per 1000 neonates are found to be birthed with some degree of brachial plexus injury, however, 80-90% of these will be expected to regain full functional mobility and control of the flail/desensitized arm by the age of 3 Months old [8]. This is combined with 1 in 100 American adults suffering from a degree of BPI– cases of which have increased dramatically over the past 50 years with the increasing use of motorized vehicles [9]. Depending on the extent of damage, location or the patients' preference there are several treatments.

1.31 Surgical Suturing and Nerve repair (Neurotisation)

Treatment for BPI since its discovery has been notoriously difficult, often requiring surgery and a lifetime of corrective therapy and rehabilitation. Historically, the first treatments involved electrotherapy, massage and employed aided passive movements. However, Kennedy et al. determined that the efficacy of these therapies were 'doubtful'. Kennedy went on to pioneer the first true treatment in 1903; exposing and suturing damaged nerves using catgut. This was a breakthrough in BPI treatments and led to restoration of sensation and motor function in 3 out of 3 cases [10]. This work was continued with experimental nerve surgery by Sever in 1916 [11] and Wyeth/Sharp in 1917 [12]. However, after this there was a distinct lack of research into BPI before 1950's possibly due to the poor results of nerve suturing in the Sever paper; regardless, Vlupius and Stoffel managed to complete the first nerve reroute in 1920 by the rerouting damaged fascicles of the pectoralis major into the musculocutaeneous and axilliary nerves to reproduce sensation [13]. It wasn't until the mid-1980's that further developments were made in nerve repair with leading scientists such as Narakas, Allieu and Brunelli making bounds in the discovery of new microsurgical techniques [14-16]. This further paved the way for neurotisation – the transfer of a nerve (allograft or otherwise) from a relatively unimportant muscle to a more valuable tissue that has lost innervation. Gu et al. in 1989 was able to autograft the musculocutaeneous nerve in 125 patients – in which 85.6% of patients regained a 'motor grading' of M3 (see Table 2).

Motor Rating	Result
M0	No contraction/Full Paralysis
M1	Trace EMG/ No movement
M2	Movement at joint with gravity eliminated
M3	Movement against gravity possible
M4	Subnominal movement against resistance
M5	Normal Strength

Table 2 shows the standard 'Seddon' table in which muscle weakness in a patient can be graded. The grading system operates from M0-> M1; representing no strength to normal.
SOURCE: Seddon HJ. A classification of nerve injuries. Br Med J 1942; 2:237-239

The Oberlin technique is the most modern, and widely accepted, form of neurotisation. This technique involves the transfer of ulnar nerves from the lower branches of the plexus and used to replace upper avulsed nerves [18]. This has been used to great success; producing M3 and M4 results in bicep strength in 94-100% and 75-95% of patients respectively [19- 20]. However, procedure has been recently associated with some mild neurological conditions such as paraesthesia – pins and needles – however this issue appears to resolve within 3 months [21].

1.32 Shoulder Arthrodesis

Throughout the 20th century there have been numerous other techniques used to treat BPI. Shoulder fusion, also known as shoulder arthrodesis, is an extra-articular technique in which the glenohumoral joint is fused by surgical pins; effectively pinning the humerus of the upper arm to the Subscapularis bone of the shoulder (see figure 5). Shoulder fusion is only indicated in cases where the patient has reached skeletal maturity and is not likely to suffer any glenohumoral growth retardance. This technique allows slight control over the patients' ability to adduct/abduct the shoulder angle (usually up to around 60 degrees) by the transmittance of force from undamaged/unaffected muscles to the humerus, often the scapula muscles [23].

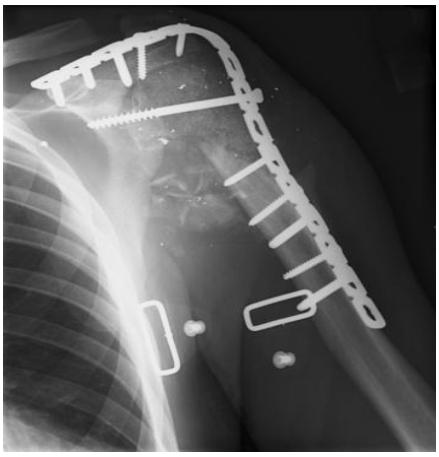

Figure 5 shows an example of the shoulder fusion technique; the pins connecting to the humerus (upper arm) and the subscapularis (shoulder) can be clearly seen which allows the transmittance of force. Through the glenohumoral joint is a pin with a loaded spring attached, allowing a certain range of movement.
SOURCE:Zsoldos et al. 2013 [22]

Shoulder fusion has been used since the 1950s to great success in restoring shoulder movement, preventing the need for amputation due to flail arm, and reducing pain from secondary conditions which can often arise from a plexus injury; shoulder contractures [4], winged scapulae [5] and subluxation [6] are all common in BPI patients. In a study by Wong et al., 83% of patients would report lessened pain and discomfort [24] and 65% of patients in another, larger, study [25]. However, it is not indicated in deeper plexus injuries from C7-T1 as it does not restore elbow flexor/extensor movement, skin sensation or hand function. Additionally, according to a study by Rorabeck et al., there has been no medical advantage for shoulder arthrodesis when compared with that of a transhumeral (above arm) amputation, in that either procedure carries the same benefit in terms of pain minimization and shoulder control [26]. Therefore it would be up to the patient to decide whether they would prefer joint arthrodesis or a prosthetic forearm.

1.33 Tendon Transfers

Recently, tendon transfers have been replacing shoulder arthrodesis as a favourable alternative; reducing pain and secondary ailments whilst still maintaining a large degree of mobility [27]. This procedure involves the relocation of a specific tendon unit to act as a substitute where another muscle has proven irreparable, and has recently been proven to be very successful. Elhassan et al. in 2010 was able to transfer a trapezius tendon to restore external rotation of the shoulder, and suggests that in addition to the trapezius, rhomboids, latissimus dorsi, pectoralis major and teres major muscle groups can prove to be equally useful in restoring shoulder function and reducing subluxation (the humerus falls out of the glenohumoral joint) and pain [28]. Transfer of the latissimus dorsi was completed by using the L'Episcopo technique (anterior rerouting of the latissimus dorsi to the humerus) in several recent key papers; in one study, 90% of patients resumed working life and produced up to 90 degrees of elevation [29-30].

1.34 Muscle Transfers

Often used in conjunction with tendon transfer, FFMT's (free-functioning muscle transfers) are often indicated 9-12 months post-trauma if there hasn't been significant progress after a neurotisation or a tendon transfer [31]. This technique involves the transfer of muscle using 'microvascular anastomoses '– surgical re-joining of blood vessels - in order to introduce a new muscle to replace the function of an impaired muscle whilst providing oxygenated blood and neural stimulation. This encourages a microneural readjustment and allows the ability to train movement whilst bypassing impaired musculature/nerves [32]. In adults with BPI, lower plexus injury and residual paralysis remaining after the uppermost roots have recovered is particularly uncommon [33]. However, it can occur – giving useful use of wrist and elbow extension/flexion but with extremely limited finger/thumb movement. In these rare cases, Muscle transfers can outperform both neurotisation and tendon transfers in terms of rehabilitation [34].

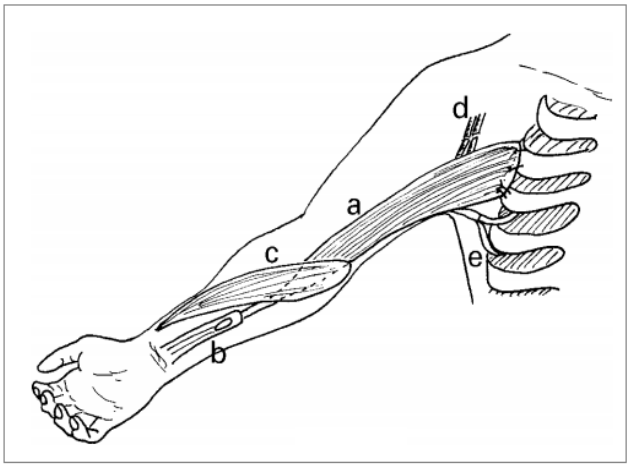

Figure 6 shows the free muscle transfer conducted by Doi et al.;
a) The Gracialis muscle implant
b) long finger tendons
c) pronator teres and wrist flexors acting on a pulley on Gracialis innervation.
d) Thoracodorsal Artery and vein used to introduce blood to the transplanted muscle
e) Third and Fourth Intercostal nerves used for innervation of the Gracialis muscle.
SOURCE: Doi et al. [35]

For example, Doi et al. used the FFMT technique into transfer the brachioradialis (forearm) to the radial wrist extensors – restoring finger flexion. Thumb extension was then achieved by transferring the forearm wrist flexors, and full thumb and finger extension was obtained by suturing the Gracialis muscle of the leg to the 2nd and 3rd ribs (proximally) and distally to the forearm – see figure 6 [35]. In all three cases where Doi et al. used muscle transfers each patient's arm mobility had improved to either M4 or M5 according to the Seddon motor function classification, with an active range of finger movement between 70/110 degrees and the ability to pick up objects up to 7Kg.

To date, muscle transfers have been greatly successful in restoring some amount of movement to a majority of patients. However, they require extremely high levels of knowledge and expertise on behalf of the surgeons – they are also exceptionally time consuming and results are not always perfect [36].

In contrast, there is another therapeutic method for the treatment of BPI that does not require extensive and precise surgery, are comparatively cheap and yet can provide strong results in the restoration of movement and rehabilitation of the nervous system in postganglionic nervous injuries – Orthotics.

1-4 Orthotics in Brachial Plexus Injury

In many cases of brachial plexus injury, often medically and subjectively, amputation followed by arthrodesis of the shoulder and rehabilitation with a prosthetic device proves to be the best option. There is a whole range of state of the art prosthetic limbs on the market which provide the comfort, range of motion and therapy a patient would desire [37]. This coupled with the fact that the standards of prosthetics are constantly rising suggests that this should be the procedure most sought-after. This is not the case. Many people given the choice of amputation versus rehabilitation of their own limb will often choose the latter even when faced with a worse prognosis – and in cases of postganglionic BPI's (i.e. regenerative) this is possible with orthotics [38].

Orthotics have been used throughout human history – beginning with simple braces and splints [39], however it wasn't until during World War 2 and after that demand rose greatly due to injuries sustained during wartime and large outbreaks of polio (causing post-poliomyelitis – a similar muscle weakness condition similar to BPI) [40]. Since the 1940's orthotics have progressed from cumbersome, unattractive and heavy rudimentary supports to highly advanced, lightweight and reliable rehabilitative devices [41]. In modern day orthotics, orthotics can be generally split into two main categories; passive and active.

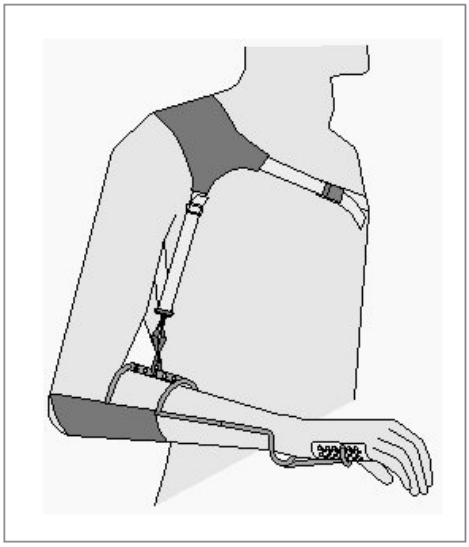

Figure 7 shows a diagram of the WILMER™ carrying orthosis, note the shoulder strap 'pulls' the humerus vertically – repositioning the humerus into the glenohumoral socket. SOURCE: CASCADE-USA customer datasheet

1-41 Passive and Active Orthotics

Passive orthotics such as the Wilmer orthosis (figure 7) are used when it is not necessary to actively aid movement, but instead provide resistive forces to prevent movement. The Wilmer orthosis is widely used in cases of flail arm (a unilaterally paralyzed arm) and allows for passive suspension of the forearm. This suspension combats subluxation – a common secondary condition where the humerus 'falls out' of the glenohumoral joint which causes pain and further loss of function. Additionally, it passively supports the wrist – preventing hyperextension – and allows internal/external rotation and use of the fingers. In both of these examples, the Wilmer orthosis is providing a 'breaking' mechanism to prevent the weight of the arm pulling the humerus out of the glenohumoral joint [42].

Active orthotics are typically much more complex by design as they often have to use complicated computing algorithms to produce movement in multiple degrees of freedom. Generally they are powered by an external power source which adds energy to the system to aid in motor function. These types of orthotic are exceptionally useful in rehabilitation, as by aiding the arm in movement they can encourage nerve regrowth and prevent muscle atrophy in postganglionic BPIs. This process is known as neuronal plasticity, where exercise can induce a

neuronal restructuring – this is a progressive phenomenon and requires repeat sessions at a slowly decreasing level of assistance to occur [43]. Often the magnitude of neuronal regeneration will rely on the patients' dedication and the time post injury in which therapy commences – Robinson et al. finds 6->8 weeks post-injury is the ideal period within which to begin neural restructuring [44].

In 'active orthotics', a device is required to generate the movement – this is known as the actuator which is typically hydraulic, pneumatic or electrical-motor driven. These types of actuator allows adjustment of the amount of aid in movement allowing for a gradual reduction in assistance as the patient 'learns' how to reuse their arm. There is a large number of active orthoses on the market that use a variety of different actuators to different ends; only a few of which will be detailed in this review.

1-52 Types of Active Orthoses

Active rehabilitation using a robotic exoskeleton is a relatively new field with the first active exoskeleton, a set of pneumatically powered legs, being designed in 1972 by the Belgrade Orthopaedic Clinic [45]. Since then, there has been a surge in new technologies in the design of active orthoses that break the mould in terms of degrees of freedom, reliability, efficiency and form of actuator. In modern day active orthoses, there are three main forms of actuation that is currently employed; hydraulic, pneumatic and electrically-driven motors.

1-52.1 Hydraulic Active Orthoses

Hydraulic orthotics use hydraulic fluids – such as oil – to create a pressure gradient in a cylinder. These gradients drive a piston forward/backwards; giving movement in either direction. Modern technology has reduced the necessary size of hydraulic systems, providing the capability to generate large amounts of power from a relatively low mass and low weight actuator. A good example of a modern hydraulic system is the FFA (Flexible Fluidic Actuator) designed by Pylatiuk et al. in 2009. The actuator (figure 8) operated on the principal that upon pressure increase via fluid valves, the actuator would expand and due to its placement on an elbow-like lever this expansion would cause flexion of the forearm. Likewise, upon pressure decrease, the actuator would contract – allowing extension. This actuator was later used as the elbow joint in a rehabilitative elbow orthotic [46]. Wiegand et al. designed a similar hydraulically powered elbow, which instead employed a fan-shape based around the same concept of a 'rotational' pressurization (see figure 8) [47].

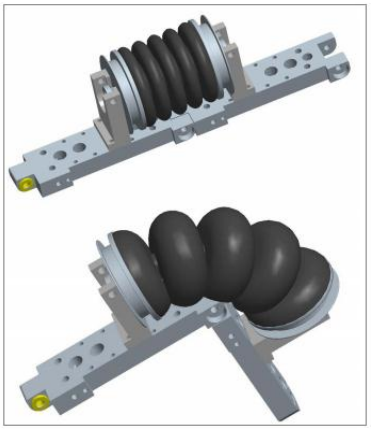

Figure 8 shows the miniaturized flexible fluidic actuator designed by Pylatiuk et al.
SOURCE: C. Pylatiuk, A. Kargov, et al. 2009 [46]

Figure 9 shows the design of the Wiegand hydraulic actuator
SOURCE: Wiegand, R et al. 2011 [47]

1-52.2 Pneumatic Active Orthoses

Pneumatics, to put it simply, is the same concept as that of hydraulics except using the energy stored in compressed air to create movement upon release and recompression; the 'outstroke' causing extension and the 'instroke' returning the piston to its original, compressed, position. These actuators, much like hydraulics, can also provide an exceptionally high power-to-weight ratio. However, It wasn't until recently with the development of Pneumatically-Actuated-Muscles (PAMs) that pneumatically powered exoskeletons could become a real option when compared to electrical or hydraulic actuators. Compared to other styles of pneumatic actuation, such as cylinders or bellows, they are extremely light and flexible. They are made with a flexible mesh membrane – but are able to transmit the same amount of power as a cylinder in a smaller space [48].

Each end of the flexible mesh membrane is fitted to opposite ends of to the component that they will transfer power to, and will bulge outward upon inflation and squeeze inwardly upon deflation – much like an organic skeletal muscle tensing or flexing (see figure10).

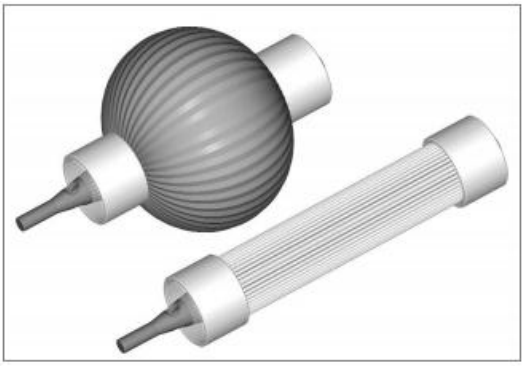

Figure 10 shows the pleated PAM developed by Daerden. Figure 10 shows the two different states of a PAM; both inflated (bulging) versus deflated (compressed).
SOURCE: Daerden et al. [51]

There has been numerous developments of different types of PAMs based around the same concept, the McKibben muscle [49], the Sleeved Bladder Muscle by Beullens [50], the pleated PAM by Daerden (figure 10)[51], the UPAM [52] and many more [53-56]. Although variants of the same concept, there are many minute details such as operation in terms of Underpressure vs. overpressure, the size of PAM and the intended use of the PAM.

1-52.3 Electrically-Driven Orthoses

Electrical Orthoses typically use a battery/mains powered AC or a DC motor to generate an assistive movement. This movement is driven when electricity is fed through the motor and causes a magnet to turning between the magnetic north and south poles within the motor. The speed of this rotation is dependent on the magnitude of the power that is being supplied. This rotating magnet, in turn, transmits this rotational movement to an axle. The main issue with electrical motors are that they rarely produce a large amount of torque on their own, and will often require extensive gear trains to increase torque – often increasing the mass and weight of the orthotic. Typically DC motors are used more often in orthotics as they have better speed control than AC motors.

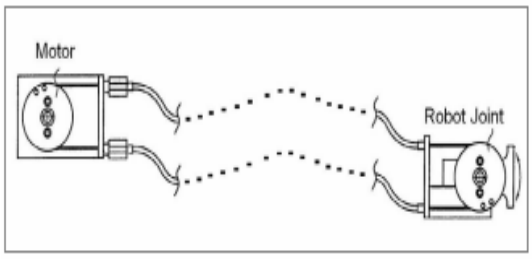

Figure 11 shows the Bowden Cable Gear transmission which was one of the first forms of electrical actuation; where a motor rotates, transmitting the torque to the joint via a cable.
Source: Schiele, A et al. 2008 [57]

1-63 Myoelectric Orthoses and Portability

A key difference between many active orthotics, independent of actuation mechanism, is that of portability. For example, the ARMin™ design described by Nef et al. is a state of the art highly advanced robotic exoskeleton which allows 6 degrees of freedom and is equipped with numerous force sensors and different modes of rehabilitation [58]. This is an exceptionally capable device with the possibility to rehabilitate many nerve conditions such as stroke and BPI. However this design, like many others currently on the market such as the Inmotion arm™ [59] robot and the Armeospring™ [60], lacks portability. These devices are large, cumbersome robots which may require attachment to a wheelchair (such as the Orthojacket™ [61], or for a patient to make regular visits to a laboratory to undergo a few hours of therapy a day/week (Inmotion arm™ [59] and Armeospring™ [60]). Additionally, these devices require an attending specialist to direct the therapy and remotely control the level of assistance the patient is receiving.

These devices are exceptionally useful for patients whom require large amounts of supervision and rehabilitation in multiple degrees of freedom; however, many BPI patients may only require aid in the extension and flexion of the elbow. For these patients there is another possibility of rehabilitation. An orthotic that was wearable, comfortable, battery-powered and simple to operate would reduce the need for extended hours of laboratory visits or supervised rehabilitation. A user would be able to use it throughout the day – personally adjusting levels of assistance to suit their rehabilitative needs.

These types of wearable orthotics designed for home use are typically known as a ‘Myoelectric Orthotic’ first designed in 1948 by Reihold Reiner [68]. Myoelectric orthotics typically use Ag/AgCl electrodes placed on the biceps and triceps muscles to measure EMG (electromyographic) signals that originate directly from EEG (electroencephalographic) signals from the brain. In essence, when the brain thinks of a specific degree of contraction of the muscle, a certain level of EEG signal is produced. This electrical EEG signal travels through the nervous system and innervates the muscle which can be recorded as a EMG signal of a certain voltage across the skin. In the postganglionic BPI patient, this signal is hugely reduced, but often traces can be picked up [62].

A patient would then have to undergo myotesting in order to determine arm locations which produce consistent signals in the biceps/triceps, and Ag/AgCl electrodes would be directly placed in these locations. A current-market example of this orthotic would be the mPower 1000 which fits as a sleeve on the patients arm which has specifically placed electrodes, which pick up the EMG signal, amplify it and correlate it to a certain degree of contraction (flexion, if the biceps is signalling or extension, if the triceps is signalling). The exoskeleton is then driven by an electric motor, which moves the arm to the ‘desired’ location [59]. Due to the nature of BPI, patients can have wildly varying EMG values corresponding to different degrees of flexion – for this reason, patients must therefore have orthotics tailored to suit their needs.

Chapter 2

Design Requirements and Aims

2-1 Aims and Critical Analysis

The aim of this project is to produce a novel prototype of an active orthotic, which conforms to the targets listed below for adults suffering from a range of brachial plexus injury.

Tsagarakis et al. stipulate that there are seven requirements for an orthotic to fulfil the aspirations of both the patient and the medical community [63]:-

i) The mass must be low, less than 2kg to avoid disturbing function
ii) Accurate compensation for external forces
iii) Safe operation and proprioception for the patient
iv) Reliable in environments where water or grease may be present
v) Low complexity/maintenance and low engineering/construction costs
vi) Simple donning and doffing of the orthotic
vii) Must meet variable resistance targets

There are numerous current-market active orthotics that meet these requirements, from research there are still some remaining points that must be addressed in addition to the 7 requirements from Tsagarakis et al. that would be beneficial to the patient:-

viii) Portability and Battery-Powered
ix) Mass producible and adjustable to accommodate the 90^{th} percentile of patients
x) Removal of Subluxation

After research, it is believed that there is not one singular orthotic that is commercially available that meet all of these targets; many orthotics suffer from complexity, expenses or engineering-costs. This paper will describe the design and construction of a novel, low cost and active orthotic that is able to conform to the requirements as stated above.

The work presented will first consist of a detailed critical analysis on actuation, component choice and material used and how they are applicable to the above. Following this will be detailed theory work showing how the proposed orthotic will work both mechanically and electronically. The report will conclude with an evaluation of the designed orthotic, and whether it meets the above design requirements.

2-2 Evaluation of Actuation

In order to progress, it is first necessary to compare and analyse the prospective forms of actuation and decide which is most suitable in terms of the 10 points listed in Section 1-7 of this report.

2-21 Pneumatic Actuators

Pneumatic orthotics, especially with the recent advent of numerous pneumatically actuated muscles, would at first appear to be a good choice. PAMs have a very good power to weight ratio where the actuator has very low mass and flexibility. Additionally, they have exceptionally low power requirements in order to compress/decompress; meaning that they do not need a torque amplifier – which is often an expensive issue with electric motor drives. However, the main downside with PAMs is that there is a requirement for a large pneumatic air supply. This would be perfect for a patient constricted to a wheelchair, but is not suitable for a wearable, portable, daily-use orthotic. Furthermore, pneumatic devices are solely contractile devices – meaning only one plane of movement. This would then require two antagonistic actuators reducing efficiency and thus increasing complexity [64]. Numerous case studies have also reported the short life span of certain PAM types – with many users complaining of fracture [65].

2-22 Hydraulic Actuators

Hydraulic systems have all the benefits of pneumatic orthotics; high power-to-weight ratio, low mass and low power requirements without the need for a large air-pressurized container. Also by using a 3/2 valve as described in the paper by Pylatiuk et al. it is also possible to have a singular actuator that controls both flexion and extension [46]. However, the use of fluid increases the complexity of the device dramatically – requiring numerous valves and a firm understanding of fluid dynamics in order to calculate the fluid volume and valve sizes required. These components can also be expensive, as the miniaturized fluidic actuators that are needed for a device such as this are in their infancy and are not commercially available – both Pylatiuk et al. [46] and Wiegand et al. [47] designed and customized their own flexible fluidic actuators. In addition to this; the flow rates and therefore the speed and force of flexion/extension are based on the hardware of the device and are not adjustable to meet variable resistance targets on one orthotic without the switching and replacing of valves.

2-23 Electrical-drive actuators

Electrical-drive motor orthotics generally employ a DC motor in order to convert electrical energy into useable rotational torque; this mechanical torque from a motor alone is often low and requires the implementation of torque-increasing gear mechanics – often substantially increasing the weight and mass of the device.

Another key issue with electrical drive motors is the lack of compliancy – the ability of a motor to understand where it is positionally. Both pneumatic and hydraulic systems have an inherent compliancy as they will achieve the correct pressurization (up to a maximum pressure) regardless of external load – obtaining the desired placement. However, hypothetically if a motor is programmed to 'understand' that a torque of 6Nm over 3 seconds is required to achieve 20 degrees of movement; it will produce this movement regardless of external forces and 'assume' it has produced the correct movement. In this scenario, a motor will produce the desired torque over time – but due to an external force will achieve a lesser degree of movement. This – if implemented without mechanical stops – may lead to overextension or flexion and potentially may harm the patient.

Due to the prevalence of electric motor-driven orthotics on the current market, there are a number of different types which achieve flexion and extension in different manners; the main forms of actuator that will be reviewed will be the worm drive system, a series elastic actuated system and the MACCEPA (The Mechanically Adjustable Compliance and Controllable Equilibrium Position Actuator) system. The three actuator models that will be detailed in this analysis also have methods to circumvent this lack of inherent compliancy.

2-23.1 The MACCEPA system

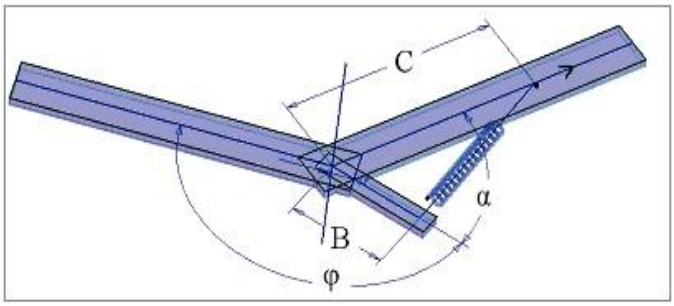

Figure 12 shows the 3 main lever arms of the MACCEPA system; the left body would be placed on the upper arm, the right body would be rotated by the primary servomotor and the small lever arm acts as a pretension mechanism to obtain compliancy. SOURCE: Van Ham et al. 2006[67]

The MACCEPA system was designed by the Vrije Universiteit Brussel in Belgium in 2009, and has been implemented to great effect in numerous gait-rehabilitative studies such as the ALTACRO robot designed by Cherelle et al [66]. The MACCEPA system (seen figure 13) is a small motor driven unit consisting of a DC motor, a planetary gearbox and two gears to increase torque– typical of many electrically actuated orthotics. The stand out factor of the MACCEPA system is how it obtains compliancy – the system does this by having a secondary independent servomotor providing tension on a spring attached to a separate small lever arm of the system .On this servomotor, it is possible to 'set' an equilibrium level of desired tension on the spring. Upon torque generation by the primary servomotor, a torque will be loaded upon the spring which will attempt to level the right body with the lever arm – where equilibrium will be reached upon when the desired degree of movement has been reached [67].

2-23.1 THE MACCEPA SYSTEM (Cont.)

This small, compact design has not yet been implemented into an elbow orthotic; however it would appear suitable as it gives the wearer the desired variable resistance targets and assistance required. Although, for the purposes of this paper, the price of two servomotors and the construction costs of engineering the many components (see figure 14) required to create a MACCEPA system outweighs the benefits. Key points stated in section 2-1 of this paper determines that the proposed orthotic must be simple, with low maintenance and low cost.

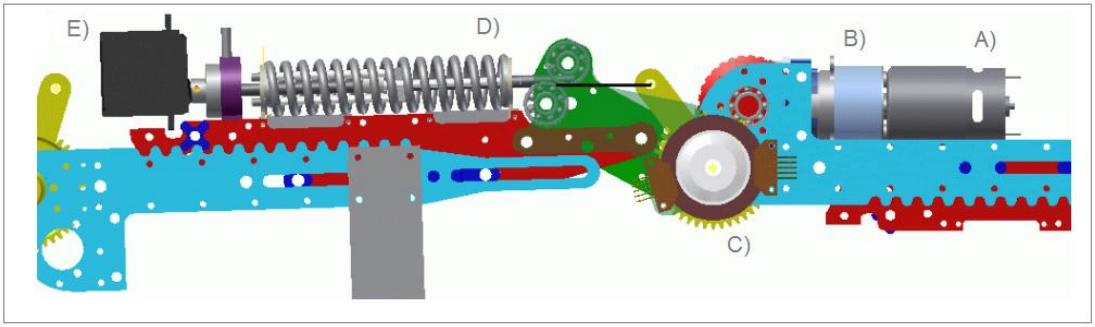

Figure 13 shows the mechanical components of the MACCEPA system; A) the motor, B) The Planetary Gearbox, C) Gear Train D) Torsion Spring E) The Secondary Servomotor
SOURCE: Vrije Universiteit Brussels, Belgium Robot and Multibody Mechanics workshop

2-23.2 SERIES ELASTIC ACTUATORS

Series elastic actuators, as opposed to the MACCEPA system, are a single DC motor electrical drive system. It, like other electrical motors, requires a large degree of torque increase via gear drives. SEAs provide several benefits when used in an orthotic; high force accuracy, low impedance and good force control within a certain bandwidth. This bandwidth is determined by its compliant component; a spring. The spring is connected in series with the motor and the lever/gear train it is acting upon [69]. In order to obtain compliancy, a position sensor is required to measure the level of actual deflection of the spring compared with expected deflection – calculated using Hookes' law:-

$$\boldsymbol{Spring\ Force} = \boldsymbol{Spring\ Constant}\ (\boldsymbol{K})\ .\ \boldsymbol{Spring\ extension}\ (\boldsymbol{X}) \qquad \textit{Eq.1 - Hookes' law}$$

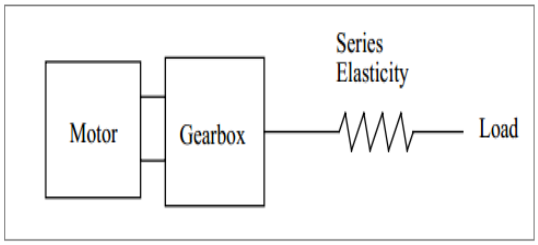

Figure 14 shows the box diagram of a series elastic actuator, with the spring connected in series with the motor, placed after a gearbox to reduce backlash.

In-built software would then calculate the force generated and the expected spring load. If this spring load is not what is expected, the motor is programmed with a control loop to determine if more or less force is required to reach the desired degree of flexion; providing the ability to compensate for external loads on the arm. Additionally, the addition of the spring after the (often) necessary gearbox can reduce friction, electronic noise and backlash [70].

2-23.2 SERIES ELASTIC ACTUATORS (cont.)

However, the main downside of the use of SEA's that will prevent its use in this project is that the spring has a set bandwidth –after which it loses its compliancy. As every commercial spring has a set stiffness constant (value K in the Hookes' law), the spring will only extend so far from zero until readings become inaccurate or the spring itself is damage which may occur when higher torques are produced – for example under a heavier external load. A study by Carpino et al. had to implement the use of multiple elastic spring components to spread the load to prevent possibility of fracture [71]. This downside combined with the prices of the additional recording equipment – such as the high resolution encoders used in the design by Kong et al. [72] – makes the SEA an actuator that would provide the desired result that is required but at a large monetary cost.

2-23.3 Worm Gear Drive

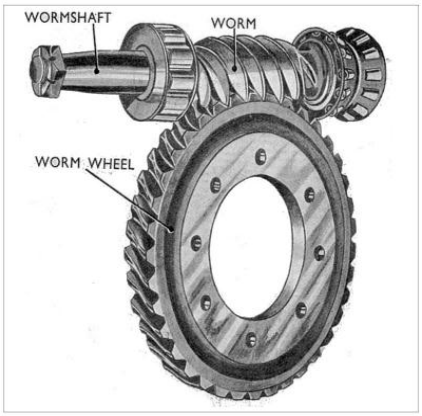

Figure 15 shows in detail the three components of a worm drive; the wormshaft, the worm and the worm wheel.
SOURCE: Manual of Driving and Maintenance for Mechanical Vehicles (Wheeled), HMSO

From l research, a worm gear drive could be implemented to the specifications set in section 2-1. A worm gear drive is a single motor drive coupled with a planetary gearbox but with a key difference – a wormshaft attached to the axle of the gearbox. The wormshaft drives the 'worm' which is a spirally-threaded screw mechanism which then directly transmits torque to the 'worm wheel' (see figure1 5). Dependant on the size of the worm/worm wheel set up this mechanism has the potential for huge gear reductions – up to 300:1 in some cases – which would drastically reduce the mass of the gear train required. This arrangement has another unique ability – the worm wheel can only be driven by the worm, and the worm wheel cannot turn the wormshaft. This means all movement is controlled by the motor, forwards and backwards, and eliminates the possibility of back-drivability.

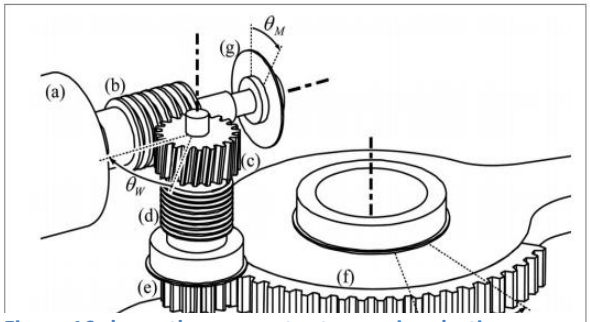

Figure 16 shows the compact rotary series elastic actuator which combines the worm drive (parts a/b/c) with a torsional spring (d) to produce compliancy and transmit force to a gear train (f).
SOURCE: Kong et al. [72]

This is a relatively cheaper and simpler mechanism when compared to other modes of actuation; however, a worm gear drive does not have compliancy – a key requirement that is needed to provide feedback to the mechanism to transmit the appropriate level of force. In order to obtain compliancy, some papers have added a torsional spring into the mechanism as seen in figure 16; but this has the same downsides as discussed with the SEA.

2-23.3 Worm Gear Drive (cont.)

Benitez. Et al designed a worm drive electrical orthotic in 2013 using the concept seen in figure 16; a worm drive actuator except without the spring as method of compliancy. This system instead used an IC-Haus-MH positional encoder with a Balluff inductive sensor to obtain positional and force control. This combination worked successfully to produce a compliant and reliable worm drive orthotic; however, these components are particularly expensive and are difficult to integrate into the system – neither of which are suitable for the purposes of this research paper.

Further research uncovered another method of obtaining force feedback and the compliancy; a Hall sensor and neodymium magnet unit. This unit, it would appear, is not particularly used in many areas of orthotics – in fact only one paper could be found using the system as an alarm system in a Lower leg orthotic to prevent overflexion and extension [73]. However, it is an incredibly cheap and reliable method of force control/feedback if programmed correctly.

A Hall sensor is a simple and reliable component that is able to pick up on magnetic fields of a certain strength and distance away from itself and transmit this data to a microcontroller as a 'tick'. Hall sensors come in many types; ratio-metric, latching or uni/bipolar. However, for the purposes of this project a unipolar Hall sensor would be perfect, as it simply 'switches' when a magnetic field enters its reading threshold. In this case, if a neodymium magnet was magnetized to the end of the worm drive and was of a certain strength to be out with the Hall sensors threshold at a maximum distance away and within the threshold at the closest distance, the Hall sensor would 'switch' on every rotation of the worm wheel. This mechanism could therefore act as a cheap, reliable encoder – providing vital force-feedback information required.

With the many forms of electrical motor-driven actuation considered, for the purposes of this project, a worm drive system combined with a hall sensor/neodymium unit can provide the low mass, compliant, adjustable system required.

Chapter 3

Mechanical Component Selection and Theory

3.1 Actuator Component Selection

A functioning worm drive actuator is made of several components; a motor, a gear train, the compliancy module and it also requires a source of power. This chapter will analyse the components which are currently on the market and select those which are applicable to the design requirements.

3.11 – DC Motor Selection

When choosing a DC motor for an application, there are a number of considerations that need to be made. The first consideration is that of the available voltage that can be used to run the motor. Due to the requirements of the microcontroller –detailed later in section 4.1 – this is a set voltage of 12V to which the motor will be matched for simplicity. There are a number of other variables that must be decided upon that depend on the application of the motor these are:-

i) Size ii) Torque iii) Power Consumption iv) Brushed vs. Brushless

v) Bearing type vi) Brush Type

i) Motor Size

Secondary to the available voltage, size is the next most important variable as it is often a limiting factor as it must fit into the space that is available. Due to the minimalist nature of this design – the smallest diameter would be the most favourable size. The two most commercially available motor diameters are 16mm and 22mm; in order to have the largest amount of complimentary non-custom gearheads, the motor would be one of these two sizes. Due to the smaller size, it would appear that the 16mm Diameter motor would be preferable. However, the chosen motor will require the aforementioned planetary gearbox, the size of which must match the motor, and 16mm diameter planetary gearboxes cannot sustain higher torques that will be required of the motor. So, in consideration of the other required components, a 22mm diameter motor is small enough for the design requirements. In this case, the Maxon A-Max series has numerous 22mm Diameter motors that have a low mass of 57g and a motor of this series will be selected for this prototype.

ii) Torque

Torque at the motor stage, in this case, is not particularly important. The A-Max series for its full range (from least to most powerful) has torques of 6.03 mNm -> 14mNm; this could be important if the designer was to use the motor by itself. However, due to the inherently low torque of the A-Max series (and all DC motors of this size) a gear train is required and therefore the difference between 6.03 mNm and 14mNm is almost negligible. Also to be considered is that the price rises when greater torques are produced.

iii) Power Consumption

Power consumption of the motor is important for the determination of the battery capacity required; a lower watt motor will require less Amps/Hour but will also change angles at a slower pace. The Maxon A-max series has motors of three wattages; 3.5W, 5W and 6W. In order to find a middle ground between speed and battery power, calculations for battery capacity were done in section 3.15 showing that 5W would provide a good power-to-battery ratio.

iv) Brushed vs. Brushless

Brushless motors typically last much longer than brushed motors – which can often rely on regular maintenance to remove dirt from the internal components. Additionally, brushless motors can also run more efficiently at higher RPMs and produce higher torques when compared with brushed motors of the same size.

However, Brushless motors have much higher power consumption characteristics when compared to brushed motors. For example, table 2 below compares two motors of the Maxon A-Max Brushed motors and Maxon EC-max brushless range of the same size and voltage:-

	Maxon A-Max 22 Ø	Maxon EC-max 22 Ø
Voltage	12v	12v
RPM	9400	12100
Nominal Torque	6.03mNm	10.2mNm
Power Consumption	5W	12W
Weight	54g	84g
Price	£32.50	£110

The minimum power consumption of the EC-max is more than twice that of the A-Max – increasing the price and size of the battery that would be required for portability. Although it produces more torque with a higher RPM – when adding a gear train this difference is almost negligible. Additionally, the price is almost triple that of the prospective A-Max motor.

For the purposes of this project, a brushed motor – although it has a shorter lifespan and may require more maintenance – would be a preferred choice in terms of cost and portability.

v) Motor Selection

Maxon A-max Ø22 mm, Precious Metal Brushes CLL, 5 Watt

Motor Type	Maxon A-Max Series
Diameter	22mm
Wattage	5W
Voltage	12V
Torque(Nominal)	6.18mNm
No load RPM	9300 rpm
Max efficiency	83%
Workable Temperature	-30 °C -> +65 °C
Bearing Type	Sleeve Bearing
Weight	54g
Price	£32.50

The motor above was selected as it fit the requirements for the motor; it is small, efficient, works in a wide range of temperature, cheap, operates at 12V and is does not consume too much power. Additionally, the selected motor has precious metal brushes which are suitable to low-current density uses – operating with low friction and high efficiency which extends the lifetime and reduces regular maintenance.

However, the bearing type uses – sleeve bearing – as opposed to the common ball-bearing type motors reduces the ability to handle high axial/radial applications. As the motor is only expected to move in one degree of freedom (controlling the elbow), it is not expected that this will be an issue.

3.12 – Gearbox + Gear Train + Theoretical Torque Output

As previously mentioned, the rotational torque actually produced by the motor alone is particularly low – only 6mNm. In a preliminary study to their design of a fluidic flexible actuator, Pylatiuk et al. found that in order for the average 70kg male to hold his forearm static against gravity requires 3.1Nm of torque, furthermore Pylatiuk et al. found that typically a non-loaded arm would experience a maximum moment of 5.8Nm in daily life – in the same study 6.5Nm was required for an average male to be able to handle a 0.5kg glass of water [74].

It would be preferable, given that the orthotic has a safe force control system capable of preventing over extension/flexion harm to the user, if the patient was able to lift heavier weights than 0.5kg for assistance in daily life. The assumption will be made that the ability of the device to maximally generate power to lift approximately 5.5Kg (including orthotic weight) would be useable for most daily tasks.

Assuming an average forearm length of 29.7cm, 17.2% of a Males (70kg height), it is possible to use the torque equation and Newton's second law to calculate how much torque the motor/gear train will need to maximally produce to generate enough torque to lift 5.5Kg. Calculations for the required torque to lift 5.5kg can be seen below in equations 3 and 4.

$$\boldsymbol{\tau = Force * Distance} \quad \boldsymbol{Force = Mass * Gravity} \qquad \boldsymbol{-----Eq.3+4}$$

$$\boldsymbol{Force = \ 5.5kg * 9.81 = 53.955N}$$

$$\boldsymbol{Required\ Torque = 53.955N * 0.29 = 16.02Nm}$$

In order to generate this amount of torque from the motors initial torque rating – 6mNm – will require an extensive gear train. A gear train transmits motion, and rotational torque from one component to another. For example, a planetary gearbox allows massive 'gear reduction' when used as part of a gear train, and will take the RPM/Torque value of the motor and increase Torque and reduce RPM speed.

This worm drive will require several components; a planetary gearbox the wormshaft and wormwheel, and a spur to translate the torque to the forearm.

By using simple gear reduction mechanics, it is simple to calculate the size ratios of the components need to generate approximately 16Nm, these components come in numerous sizes.

3.12 – Gearbox + Gear Train + Theoretical Torque Output (Cont.)

The selected planetary gearbox must complement the diameter of the motor, which in this case is 22Ø Mm. Additionally it is often simpler to buy a gearbox from the same manufacturer in order to ensure a strong connection, synchrony and efficiency between the two components. There are a number of other variables that can decide which planetary gearbox is required, but secondary to size, the input torque and maximum feed force (newtons) that the gearbox can handle is the important ones. Overstraining the device in this manner can lead to shortened life span of the gearbox and increases the likelihood of mechanical damage. In light of the 6mNm rating of the motor, the gearbox selected must be able to handle a higher rating of this number, to ensure maximum efficiency.

As mentioned previously, this orthotic will have three gear train components which must add up to approximately 16Nm. Planetary gearboxes have the largest scope in terms of gear reduction, so a large ratio at this stage would be beneficial. In order to get 16Nm, since there are components (worm wheels/gearboxes/spurs) that have varying gear reduction values, it is simply a case of picking the right set of numbers that add up to your desired output in the steps you require.

For instance, the Maxon 333:1 PG would give a torque output of 6mNm * 333 = 1.998Nm. This combined with a 4:1 worm set, providing 8Nm of torque and ending on the forearm axle of a 2:1 spur, provides the desired 16.2Nm desired in a relatively small space.

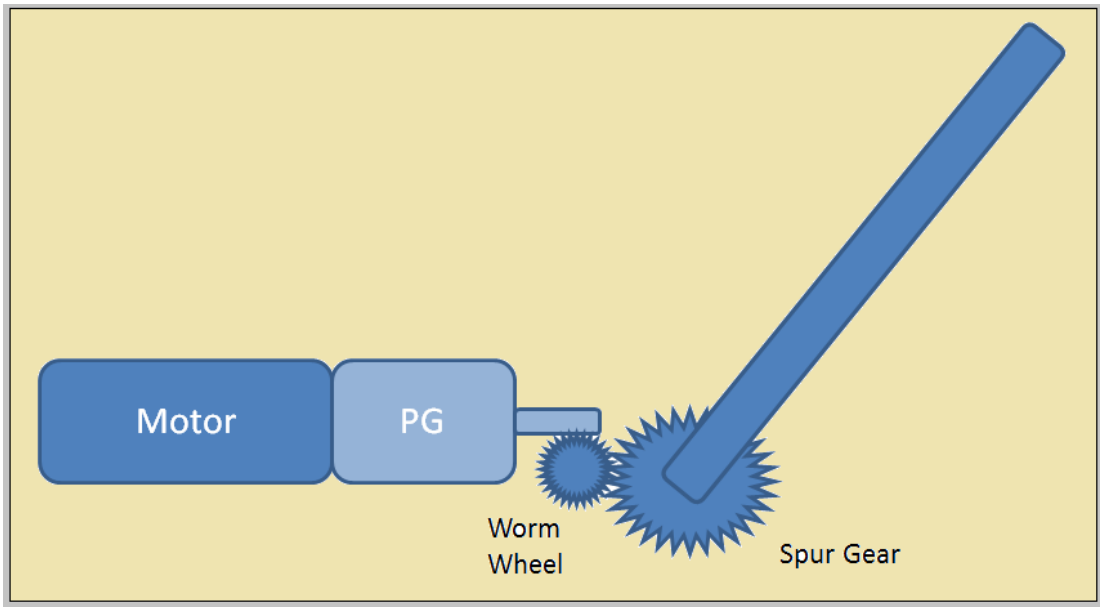

Figure 17 above shows the proposed gear train for the device. The motor directly connects to the complementary planetary gearbox, the spur of which is attached a wormshaft which drives a 4:1 worm wheel. This worm wheel in turn transmits torque to a 2:1 spur gear (twice the size), which drives the forearm axle. This should theoretically produce 16.2Nm of torque – enough to lift 5.5Kg (including the orthotic mass). Assuming less efficiency due to friction of the gear train, the patient should still be able to lift a decent weight – but this will be tested for in the prototyping phase.

3.13 – Neodymium Magnet + Hall Sensor

As previously discussed in section 2, worm gear drives do not have the required compliancy and force control that is a necessity in an orthotic. Also previously mentioned was how a hall sensor/ neodymium magnet sensor could be applied to the system to perform the necessary force-feedback required to allow the handling of external loads. This section will describe the components required, and how they will interact.

As with all components in a project like this, size is of the paramount importance. The neodymium magnet will be attached to the end of the worm gear set in order to measure the number of rotations per second, with this in mind it is easier to purchase the smallest neodymium magnet available and buy a hall sensor that is sensitive enough to pick it up. Commercially, the smallest neodymium magnet is 1x1mm and is small enough to fit on the end of the wormshaft. The full layout of the magnet/hall sensor can be seen below in figure 19. The diameter of the wormshaft (5mm) will therefore play a direct result in the magnetism experienced by the hall sensor. The magnetism can then be calculated at the furthest and closest points (of the magnet to the sensor) by using the equation (Eq.5) below:-

$$B_x = \frac{B_r}{2} * \left(\left(\frac{h+x}{\sqrt{\frac{d}{2}+(h+x)^2}} \right) - \left(\frac{x}{\sqrt{\frac{d^2}{2}+x^2}} \right) \right) \text{--------- Eq. 5}$$

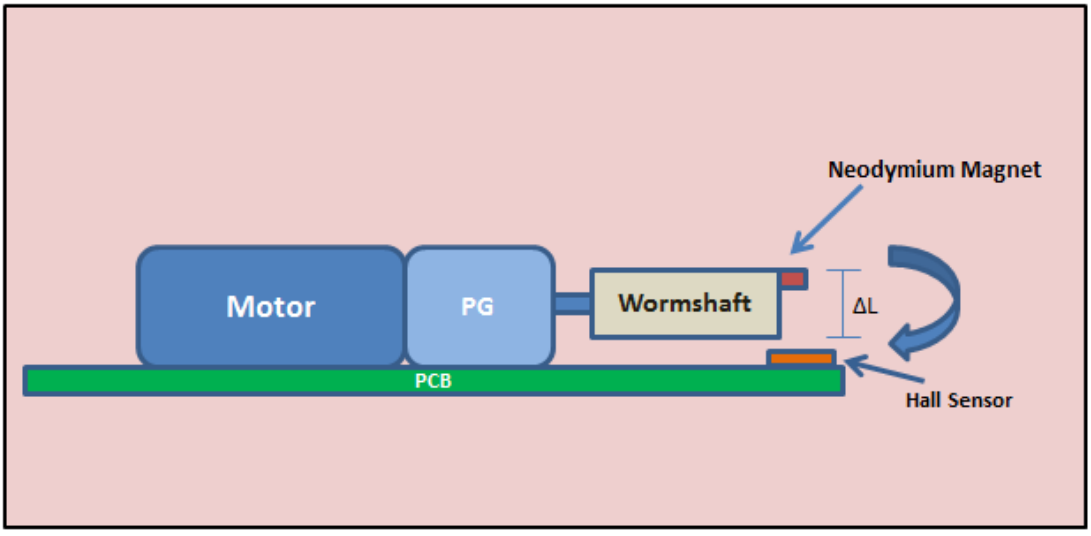

Figure 19 shows the set-up of the neodymium magnet and hall sensor in relation to the actuator system. Also seen is the PCB, the printed circuit board, on which the hall sensor will be powered by and feed information through.

3.13 – Neodymium Magnet + Sensor Unit (Cont.)

Equation 5 is the law for determining magnetic strength in a permanently fixed circular magnet. Assuming a wormshaft diameter of 5mm and a minimum distance of the hall sensor of approximately 0.4mm at the closest point (therefore 5.4mm at the furthest point), and a 1.32T N45 grade 1x1mm neodymium magnet, magnetism can now be calculated:-

Using Eqn. 5 to determine magnetism at farthest point:-

$$B_x = \frac{1320}{2} * \left(\frac{1 + 5.4}{\sqrt{0.5^2 + (1 + 5.4)^2}} - \frac{5.4}{\sqrt{0.5^2 + 5.4^2}} \right)$$

$$B_{x\,farthest} = 0.80mT$$

$$B_x = \frac{1320}{2} * \left(\frac{1 + 0.4}{\sqrt{0.5^2 + (1 + 0.4)^2}} - \frac{0.4}{\sqrt{0.5^2 + 0.4^2}} \right)$$

$$B_{x\,closest} = 176mT$$

----------	Farthest	Closest
Br[mT]	1320	1320
t [mm]	1	1
r [mm]	0.5	0.5
x [mm]	5.4	0.4
Bx [mT]	0.8	176

Table 3 shows the calculations for the magnetism experienced by the hall sensor at the furthest and closest points of the magnet from the hall sensor. Where Br = Magnetism of the Magnet in Tesla, t is the thickness of the magnet, r is the radius of the magnet, x is the distance of the magnet from the sensor and Bx is the magnetism experienced.

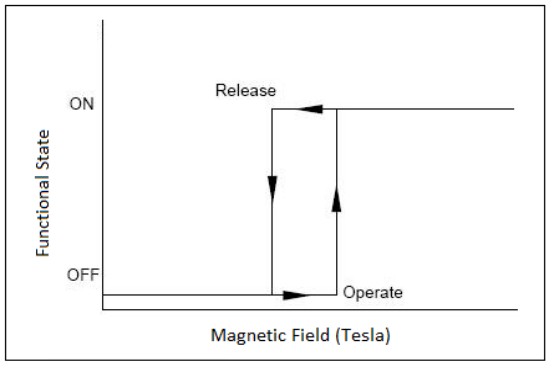

Figure 20 shows a typical hysteresis graph of a hall sensor; it only triggers upon a certain threshold, and the magnetism must flit between these two points in order to record a 'rotation' of the worm wheel. SOURCE: Honeywell MICRO SWITCH Sensing and Control, "Hall effect sensing and application."

Now that the magnetism of the 1x1mm magnet has been calculated, it is necessary to select a complementary hall sensor. The hall sensor is a simple digital switch that records when it is triggered, in this case by a nearby magnetic field. Every commercial hall sensor has a hysteresis graph such as seen in figure 20. With this in mind, it is necessary to pick a sensor that triggers when the magnetic field is above a certain threshold, and deactivates at a below certain threshold – in this case the threshold is above and below 176mT. Upon triggering, this information will feed into the microcontroller which will record as one 'rotation'. The microcontroller will also be programmed in such a manner to calculate what RPM is required to reach a specific angle, and upon introduction of an external load, how much more torque is required (if the expected RPM is not reached). The US5682 Series 24V unipolar Hall sensor in a TSOT-23 surface mount fits these specification; with a trigger point of 132mT.

3.14 – Power source

As the proposed orthotic is designed to be portable and used throughout the patients day as an assistive device, the orthotic will therefore need to have an external and easily portable power source such as batteries. In terms of self-defined requirements the battery pack must be:-

i) Easily rechargeable by the patient, using a common mains-capable charger
ii) Able to operate at an optimum level for at least 20 hours
iii) Safe in conditions the patient is likely to find themselves
iv) Of unobtrusive size and weight
v) Cost efficient

As stated above in Section 3-1, the motor that will be used will be the 12V Maxon A-Max DC 22Ø motor. To calculate the battery capacity and power needed, it is first required to consider the voltage and power consumption that is likely to be used by the motor in the time it will be in use. The motor, as stated by Maxon, has a power consumption of 5W at peak torque, a voltage of 12V and a no-load RPM of 9400. The power drain in Amperes can then be calculated using equation 6, below.

Calculating power drain:-

$$\text{Input Current} = \text{Output Power (5W)} / \text{Input Voltage (12V)} \quad \text{-----} \quad \text{Eq.6}$$

$$= 0.41\text{A}$$

Additionally, it is necessary to calculate the theoretical capacity that is required of a battery in order to run to specifications. In this report, the assumption is made that 20 hours of runtime is more than enough for a patients' day-to-day life – as it is most likely that the patient will recharge it overnight and will obtain more than four hours of sleep per night. Additionally, it is also likely that the device will run for longer, as the device will not be running at peak capacity for the full time it is in use. This is calculated using Eq.7 below.

Calculating Required Battery Capacity:-

$$\text{(Ah)} = \text{Device's Wattage (5W)} \times \text{Time to run (20 Hours)} / \text{Battery Voltage (12V)} \quad \text{----} \quad \text{Eq.7}$$

$$= 8.3\ \text{Ah}$$

In order to run the 12V motor for 20 hours – an estimate of the upper maximum of the patients' day – would require a battery of approx. 8.3Ah. A battery pack will now be selected with this specification in mind.

3.14 Power Source (cont.)

There are numerous brands of batteries on the market to consider that range from very cheap to very expensive – all used for many different applications. However, these can be boiled down to 5 main types of battery that can be considered for use in this project; the lead acid battery, nickel cadmium battery, Nickel Metal Hydride, Lithium Ion and Lithium Polymer.

All types of rechargeable batteries would theoretically work in the proposed orthotic, however there are key differences in size, cost and power-to-weight ratio. Out of the 5 options, lead acid batteries are the cheapest but largest form of battery. For this project, size and weight is of paramount importance to the user as it must be comfortable to wear and not interfere with the patients' daily activities, as per requirements stated in section 2-1. Lithium batteries are quickly becoming the battery of choice in many electronic devices – mostly due to their small mass, high power and long shelf life (see Table 2). There are two forms of lithium battery on the market, lithium ion and lithium polymer. Lithium ion has the highest energy density (mAh/weight); however a key downside is that they have the capability to burn or explode when handled improperly – requiring protective circuit boards to prevent overcharging or overdraining. Accounting for the unsupervised nature of the orthotic, this could be a bad choice for some patients.

Lithium Polymer batteries have a slightly lower energy density than lithium ion, but the differences in terms of weight are almost negligible and the increased safety makes it a much better option. Lithium polymer would no doubt produce the best results for this project in terms of safety, comfort, mass and operating lifetime - at a price. In order to obtain the 8.3Ah rating as stated earlier, some lithium-polymer battery pack can cost less than $50, but this could increase to $150 for well-known and reliable brands.

Battery Chemistry	Weight	Operating temperature (C)	Cycle/Shelf Life	Volts per cell
Lead Acid	Heavy	-65 -> 80	12	2
Nickel Cadmium	Heavy	-20 ->65	6	1.2
Nickel Metal (NiMh)	Moderate	-10 -> 65	12	1.2
Lithium Ion	Light	-20 -> 60	12	3.7
Lithium Polymer	Light	-20 ->60	12	3.7

Table 2 above highlights the main differences between the main batteries types currently found on the market.

3.2 – Actuator Design Plans

This section will show the overall design sketches of the actuator, including size and dimensions. Figure 21 below shows the side view and dimensions of the full design and Table 13 below shows a summary of the theoretical aspects of the actuator.

3.21 – Side View

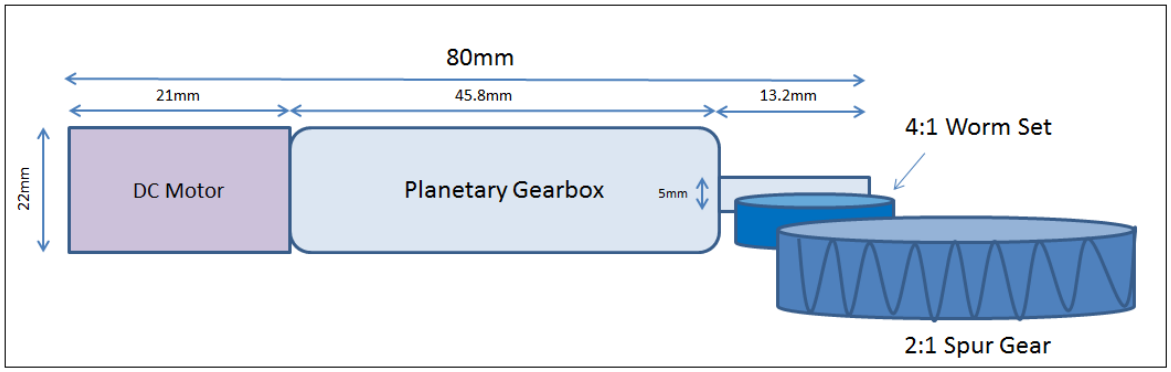

Figure 21 shows the dimensions of the Maxon A Max motor, the 333:1 planetary gearbox, the planetary axle and wormshaft, followed by the 4:1 worm wheel and spur gear described in Section 3.1 in a side view.

3.22 – Statistics

Table 3 shows a summary of the data for the full actuator as described in Section 3.

Total length of Actuator = 80mm	Total Length of Actuator + Spur set = 110mm	Total Height = 22mm	Total Height of Actuator + PCB = ~30mm
Total Weight of Actuator = 140g	Total Weight of Actuator + Full Gear Train = ~250g	Total Torque Produced = 16.2Nm	Operable Temperature (Min/Max) = -20°C to +60°C
Expected Battery life = ± 20 hours	**Total Price = £135**	----	-----

Chapter 4

Electrical Components and Theory

4.1 – Electrical Component Analysis

The aim of this section is to describe in detail how the electrical signal from the brain will be picked up in the muscle as an EMG, undergo signal processing and eventually turned into a rotational torque provided by the motor described in section 3-1.

4.2 – Proposed Circuit Box Diagram

Figure 22

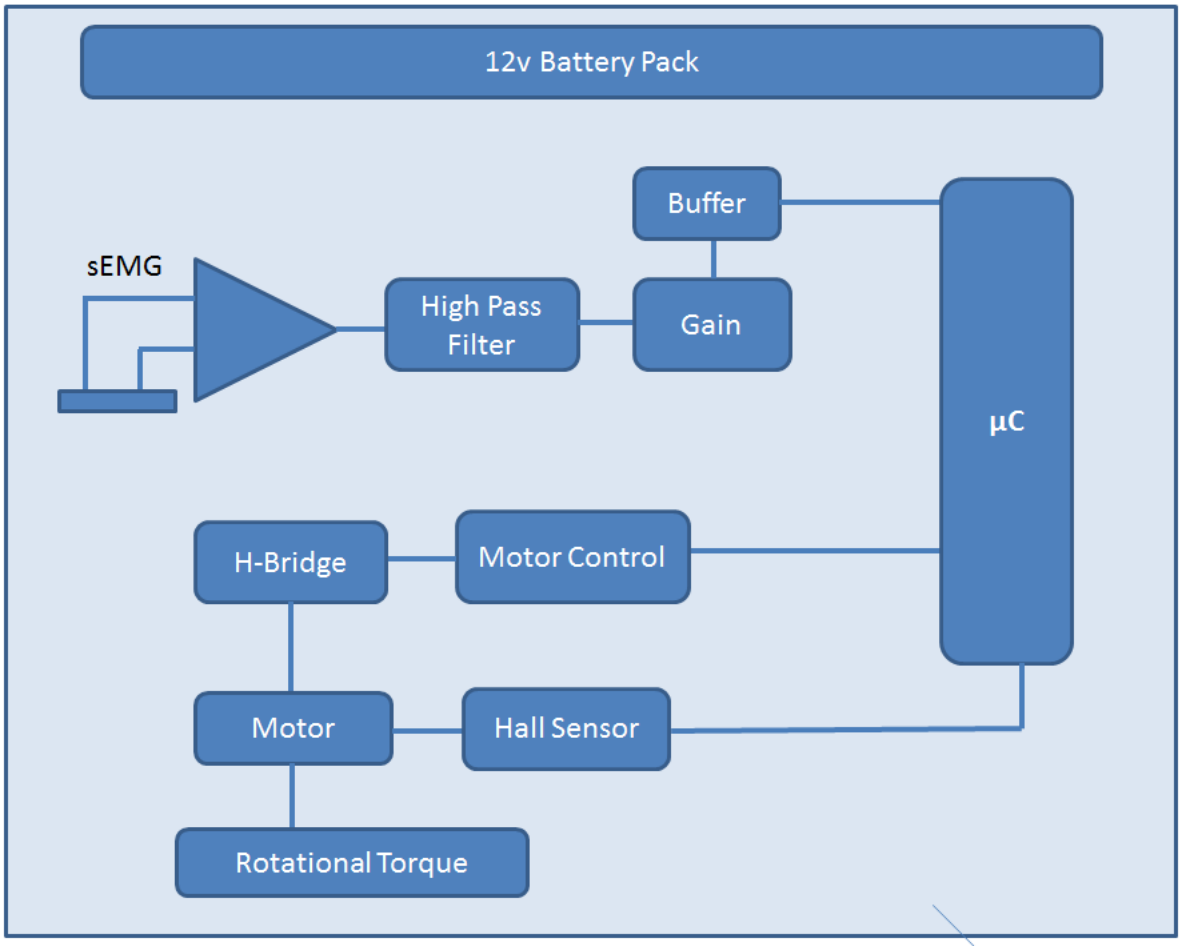

Figure 22 above is a box diagram which diagrammatically shows the proposed circuitry that will be used in the prototype; from the sEMG signal picked up by the electrodes through signal processing and filtering into a useable signal which eventually generates torque that is controlled by a feedback loop by the Hall Sensor/Neodymium magnet unit. The following sections will analyse each section individually and state which component would be suitable.

4.3 – Components and Electrical Theory

4.31 – Electrode Theory

As described in section 1, electrical signals that correspond with a degree of flexion or extension are first generated in the central nervous system which is then transmitted to the intended innervated muscle by the postganglionic nervous system. There must first be a component which detects and records this analogue signal, this component is typically Ag/AgCl or silver chloride electrodes. Silver chloride electrodes are used as they transmit a signal with 100% efficiency (source), are stable and relatively inexpensive [75]. They work like a standard electrode, taking a voltage reading between two points –in this case- on a muscle such as the biceps or triceps.

The obtained signal can vary largely between age groups and gender, even in normal patients. In healthy subjects, this signal can range of mean 10± 3.3 to on the biceps and 11±0.99 the triceps [76][77]. However, this signal is weakened and likely abnormal due to the nerve damage found in BPI patients. Placement of the electrode must therefore be perfect in a patient, so a prospective user of this orthotic will have to undergo myotesting to determine the extent of the injury, the type of injury and generate a composite study of the individuals EMG signals.

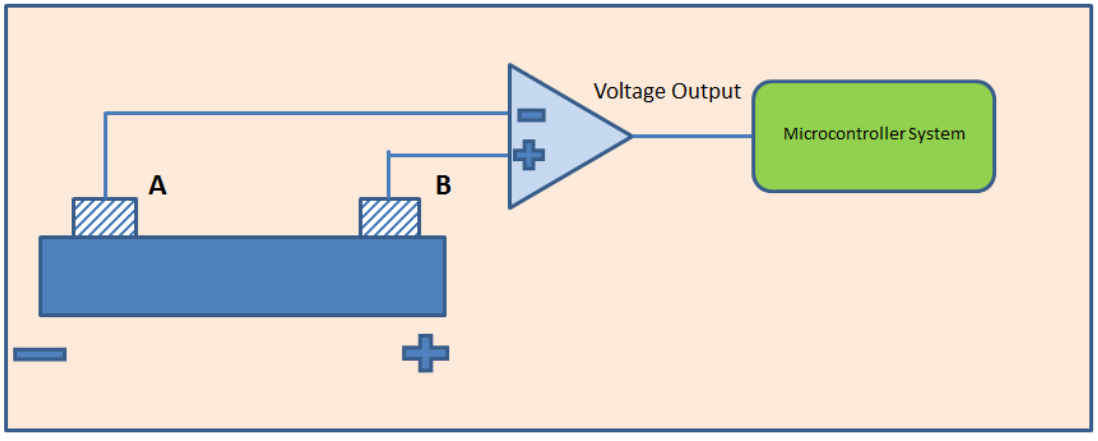

Figure 23 Shows the common electrode set up in order to detect a potential difference between two points which is then read as a value, interpreted by the remainder of the electrical system

4.32 EMG signals in patients with Brachial Plexus Injury

Typically myotesting, consisting of EMG measurements and NVG (nerve conduction velocity studies), will take place between 3-4 weeks post-injury which allows adequate recovery after the accident [79]. Additionally, if the conduction studies take place in the first 10 days, they are only capable of telling whether damage is present and may be misdiagnosed as a pre-ganglionic injury. This time period also directly comes before the 6-8weeks Robinson et al stated to be the most suitable time to undergo rehabilitation [44].

Both SNAP (sensory nerve action potentials) and MNAP (motor neuron action potentials) will be measured to determine the form of injury; in preganglionic injuries, there will be normal SNAP signals and attenuated MNAP signals. This is because the dorsal root of the sensory nerve is attached to the skin, and therefore is receiving information, but cannot transmit this into the CNS due to a pre-ganglionic detachment – resulting in paralysis. In postganglionic injuries, the opposite is true, where SNAP will be negligible or fully absent and there are weakened MNAP signals [80].

If myotesting determines the patient is a suitable candidate (i.e. has only peripheral nervous damage), further myotesting will be undertaken to identify the CMAP (the compound muscle action potential) of the biceps and triceps brachii to use a consistent (albeit weakened) signal as the input voltage for the robotic exoskeleton[81]. Typically the location of the most consistent signal will be on the middle belly of the bicep, according to a study by Wee et al, which shows the least variation in signal between genders and ages [82]. The presence of this CMAP signal within the arm indicates that some motor axons are still intact – and rehabilitation can then be undertaken. Due to measurements being taken as a compound signal, there is no exact figure for what level below 'normal' represents a definite abnormality – signals tend to vary with age, gender and level of fitness. However, a general rule of thumb stipulates that CMAP values for the biceps/triceps brachii under 50% of 'normal' represent nervous damage [83]. For figures of a normal patient, please see figure 26.

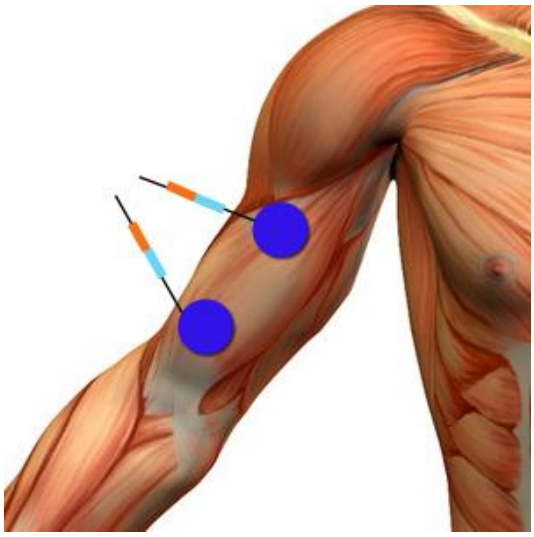

Figure 24 shows the correct placement of the biceps to generate a steady input voltage. Studies by Ahamed et al determine this to be the best location for electrode placement
IMAGE SOURCE:- Sport-Elec Institut Ltd

For the purposes of this experiment, we will consider the biceps brachii signal of amplitude 10mV, conduction velocity of 45m/sec and onset latency of 4.5ms – 50% of the values found in tables figure 26.

EMG values in normal studies – Figures 25, 26 and 27

Table 4 Sensory Motor Neuron Normal Values *

Nerve	minimum Amplitude (uV)	minimum C.V. (m/sec)	maximum Peak latency (ms)
Ulnar (wrist)	10	53	3.5
Median (wrist)	20	53	3.7
Radial (triceps)	20	48	2.7
Sural	6	41	4.2
Ulnar (palm)	–	–	2.1
Median (palm)	25	–	2.1

Table 5 Motor Neuron Normal Values *

Nerve	minimum Amplitude (mV)	minimum C.V. (m/sec)	maximum Onset latency (ms)
Ulnar***	6	49	3.5
Median	4	49	4.4
Peroneal	2	41	6.1
Tibial	3	41	6.1
Facial	1	–	4.0
Musculocutaeneous** [Biceps Brachii]	10.1 ± 3.3	38-62	4.5 ± 0.4
Radial*** [Triceps]	11.24mV±0.99	---	5.57±0.59

*Source: [78]

**Source: Mean Value [76]

*** Innervates the Triceps Brachii: Mean value [77]

4.4 Signal Processing + Components

In order to obtain a useable signal for the motor to determine an angle of flexion/extension, there are numerous steps that must be first undertaken. Many signals, especially bioelectrical signals, are either particularly low amplitude or have numerous forms of disturbances or artefacts that can make them hard to implement reliably into an electrical system. For this reason, most bioelectric signals must undergo several steps of processing. In addition to this, the motor must be programmed to react to this signal, and have a method of recognising and driving forwards and backwards movement – this all requires electrical programming.

4.41 – NOISE FILTERING

The first obstacle after picking up the surface EMG (sEMG) using Ag/AgCl electrodes as described in section 4.1 is that there are often numerous 'noises', or electrical interference, in biosignals that alter the signal greatly. These often come in different amplitudes, different frequencies and for different reasons (see table 4).

Table 6 - frequency of common interference signals

Type Of Interference	Typical Frequency	Reason
Thermal Noise	Variable	Amplification System
Chemical Noise	10Hz*	Skin Electrode Interface
Movement Artefacts	25Hz**	Muscle Contraction
Tremors	1-40***	Neuropathy-Related
Gaussian Noise	10Hz****	White Noise

*** Varying dependent on components used**
**** Huigen et al. 2000 [84]**
***** Oster et al. 1980 [85]**
****** Trenado et al. 2014 [86]**

Due to these possible artefacts, filtering is required to extract these signals from the sEMG signal. This can be done by using a high pass filter with a simple cut off frequency; however, the exact cut-off point that can be argued. sEMG signals are in the range of 1-450Hz, so it would appear that using a cut off frequency of 40Hz to block out all possible artefacts would be the best option. This is not the case; this is because the 20+Hz range contains the amplitude peaks of sEMG signals of small muscle contractions and movements [87]. For this reason, some institutions quote 10Hz as the appropriate cut off point (The Journal of electromyography and kinesiology), others quote 5Hz (International society of electrophysiology and Kinesiology) including some papers [88].

However, this fails to attenuate many of the above artefacts; a paper by Luca et al. studied sEMG using a range of cut-off values, 10, 20 and 30 Hz. At 30 Hz, the filter removed all of the potential artefacts, but 7.4 to 13% of the sEMG signal was cut. This caused the loss of many low-frequency movements and signal loss. They also found that in many neuropathic signals, where sEMGs are weakened, and cut off's below 20 Hz appear unstable [89]. Due to this, they suggest a cut off of 20Hz to be the best balance between optimal signal and attenuation of interference, a suggested backed up by other sources [90].

4.41 Noise Filtering (Cont.)

Although the tremor – a common side effect of brachial plexus injury – is rated between 1-40Hz, typically tremors are sub-10Hz; with higher frequency bands of 20/30 or even 40 much magnitudes rarer. So in this case, a high pass filter with a cut off frequency of 20Hz would be effective at producing a valid sEMG signal [87]; in this case a passive filter would be acceptable versus an active, as an active requires an external power source.

4.42 Gain

The theoretical signal that we are dealing with so far now has a frequency of 20hz – 450Hz (under extreme load), and an amplitude of 50% of 10mV ± 3.3. The microcontroller board that will be used in this project, detailed later in section 4-7, can handle and interpret input voltages of 0V-5V without hardware reconfiguration. For this reason, an instrumentation amplifier will be used to increase the gain of the sEMG electrode signals.

As mentioned above, the minimum and maximum input when taking standard deviation into account will therefore be:-

$$Minimum\ Input = \ 50\%\ of\ (10 - 3.3mV) = 3.4mV$$
$$Maximum\ Input = 50\%\ of\ (10 + 3.3mV) = 6.7mV$$

As previously mentioned, it is necessary to input this into the microcontroller, where the maximum input is read as 5V and the minimum input is 0.

$$5V = input\ voltage * GAIN$$
$$\frac{5V}{0.0067} = Gain = 746G$$

The Arduino Uno utilizes a 10-bit ADC, which allows for 1023 counts of resolution; in this case, a maximum of 5v will correspond to a full-scale reading of 1023 and 0v correspond to no input. This gives 0.0065mV per count. However, due to individual tolerances of components involved with the filtering and amplification stages – as well as noise – it is necessary to allow for a higher margin that would be theoretically expected. By increasing the margin of error for maximum inputs, it is possible to reduce computational errors and minimize something. However, increasing the upper margins also decreases resolution and voltage/per count;

$$For\ example, using\ an\ upper\ limit\ of\ 15mV; \frac{15}{1023} = 0.014mV/count$$

$$Using\ theoretical\ upper\ limit\ of\ 6.7mV; \frac{6.7}{1023} = 0.0065mV/count$$

4.41 Gain (Cont.)

As the near-maximum of a fully functioning bicep is approximately 10mV; the orthotic will be designed to handle near to this level. As such, an upper limit of 10mV will be used to allow the majority of patients to use the orthotic until almost normal strength and function has been obtained

$$Using\ an\ upper\ limit\ of\ 10mV = \frac{10}{1023} = 0.00977mV/count$$

The instrumentation amplifier that will be used to perform this is the LT1167 designed by Linear Technologies, as it provides high levels of gain (up to 10,000) with a single passive resistor whilst producing low noise – of frequency that would be blocked by the filtering high-pass filter previously described in section 4.41.

4.42 – Buffering and CMRR

The instrumentation amplifier described in section 4.41 also has a built-in voltage buffer mechanism. This is required as the original signal – the sEMG – is particularly high source impedance [91] whereas the microcontroller unit will be low impedance. The buffer amplifier contained within the LT1167 provides high input impedance followed by low output impedance – matching the impedance before and after the buffer. This will drastically reduce voltage amplitude instability – maximising the power transfer and minimizing signal reflection between the Gain stage and microcontroller stage.

In addition to the integrated buffer, the LT1167 has a very high Common-Mode-Rejection-Ratio (CMRR) of 90dB and G = 1; where a CMRR of 70dB is considered a 'good' CMRR. This value determines how well the amplifier gets rid of unwanted signals thus providing an extra layer to remove unwanted noise from the sEMG signal by rejecting a signal that is common to both inputs – i.e a steady source of interference rather than a changing sEMG signal.

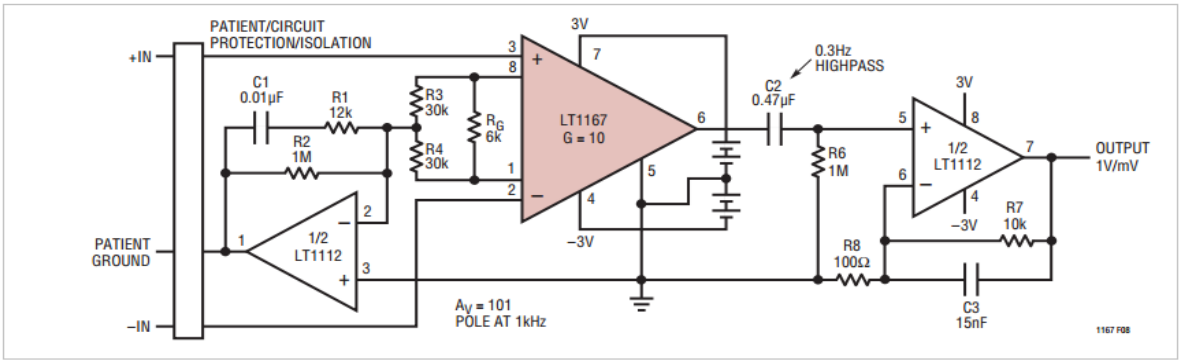

Figure 28 shows the circuitry of the LT1167 gain and LT1112 buffer amp that will be used in signal processing. As can be seen, it has a low supply voltage of 3+/- V, has an inlaid 0.3Hz High pass filter that removes the instrumentation noise of the components, and contains patient/circuit protection mechanisms to increase safety
SOURCE: Linear Technology Ltd. LT1167 datasheet

4.5 Motor Control

One of the most powerful aspects of using a DC motor over an AC motor is that of programmability and its ability to change speed quickly to a fluctuating input voltage. This section will detail the components and systems that are required to generate the varying torques and force feedback that the motor will require.

4.52Pulse Width Modulation

Pulse wave modulation is a technique used to control motor speeds where the maximum output torque of the motor is not the desired response. PWM allows varying motor speeds and, by extension, torque to be produced in response to varying input voltages.

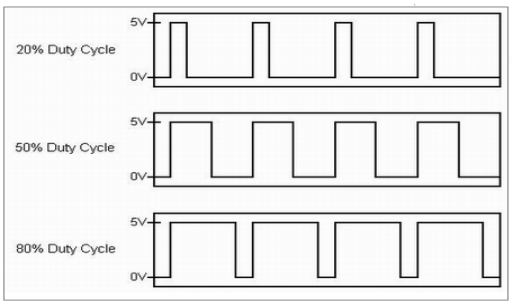

Figure 29 shows how changing the pulse width can obtain varying voltages and therefore varying torques using Pulse Width Modulation. SOURCE: NI-DAQmx PWM series datasheet

Digital circuit switches exist in a state of either on or off – in this case, if a circuit was consistently on (i.e. 5V) it would produce the maximum of 16.2Nm torque – and if the switch was consistently off (0V) then a torque of 0Nm would be produced. Pulse wave modulation is the rapid changing of the input wave – seen in figure 29. By changing the 'pulse width', you can alter the average voltage which is' seen' by the circuit. For example, if a 2.5V (8.1Nm) torque was required this would be known as a 50% duty cycle. This duty cycle is obtained by using a 1:1 mark-space ratio (figure 29) which generates 50% of power. The same can be done for any voltage between 0 and 5V to achieve the desired power.

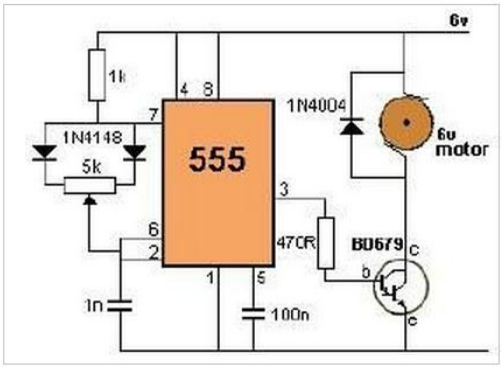

Figure 30 shows the IN555 timer circuit when combined with a 6V motor; the theory remains the same, however it would be combined with a 12V motor and a 12V rail supply.
SOURCE: NEXT Electronics Ltd IN555 Datasheet

For the purposes of this design, a simple timer switch can be used. The IN555 timer control system is a cheap commercially available component which can be used to drive the varying speeds of the motor. The circuit diagram of the IN555 with the motor can be seen in figure 30. However, this timer is already integrated into the Arduino System described in section 4-7.

4.51 H -Bridge and Directional Motor Control

The motor is designed to receive varying signals of one of two types; a signal that determines flexion (originating from the biceps) and a signal that determines extension (originating from the triceps). If pulse wave modulation controls the force of the motor, there must be another component which controls the direction in which the motorforce is applied. Commonly used for this purpose is a component known as an H bridge.

In motor control, H bridges are commonly used to change the direction in which a motor receives the input voltage. By using a specific combination of –usually- four switches, the H Bridge can reverse the polarity of the magnets operating within the DC motor. This polarity reversal leads to a directional change – resulting in either flexion or extension of the arm. This is accomplished by a series of 4 switches that are either 'on' or 'off' – resulting in a number of different outcomes. The table below states the results that occur, depending on which of the four switches are on or off – the switch configuration be seen in figure __ as they would be placed in an H bridge circuit.

S1	S2	S3	S4	Result
1	0	0	1	Flexion
0	1	1	0	Extension
0	0	0	0	Free running Motor
0	1	0	1	Motor Brakes
1	0	1	0	Motor Brakes
1	1	0	0	Shoot Through
0	0	1	1	Shoot Through
1	1	1	1	Shoot Through

Table 5, above, shows different switch combinations and their result.

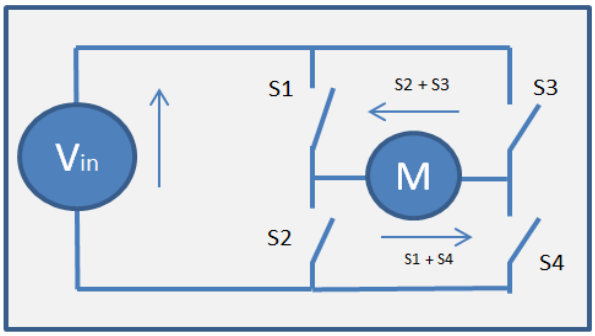

Figure 31 shows the proposed circuitry of the designed H bridge.

With this set up, it is possible to program the microcontroller to vary the switches depending on the input signal in a variety of occurrences:-

1) Signal originating from triceps; switches 2 and 3
2) Signal originating from Biceps; Switches 1 and 4
3) Position of motor at a programed stop point switches 2/4 or 1/3
→ This can act as an electronic braking mechanism to prevent overextension/overflexion

The shoot –through results is an undesirable condition that should never arise; creating a very low resistance path from the electronics to ground. In the event of a shoot-through due to a low-power input, this can result in heat production damaging the internal components or powering down the system. In a high-voltage input, this can result in a battery explosion or worse.
To prevent this, shoot-through prevention drivers can be added to the circuit for added safety.

4.53 Positional + Force Control

One of the intrinsic advantages, as previously mentioned, of using a worm drive motor is the lack of back-driveability of the worm wheel – only the motor can drive flexion or extension. Provided that the system is not hugely overloaded, it is nearly impossible for the worm wheel to turn without the motor driving it. However, the system still needs a form of force control to compensate for external loads that occur from the patient picking up items. As stated in section 3.14, a Hall sensor and neodymium magnet will be used for this function. The mechanical theory and magnetic field calculations have already been done in section 3.14, so this section will describe the electrical circuitry that underlies the concept.

As the range of movement and input voltages can vary hugely between individuals due to age, gender, or extent of damage – individual calibration is required to set reference positions of angle and expected wormshaft rotation targets. Calibration would tailor the orthotic to the individual's needs and resistance targets. The microcontroller would have to be programmed to understand what input signal correlates to what angle of flexion and how many rotations are required to achieve that angle.
The torque feedback-control program would be further designed to understand if it did not reach the desired number of rotations with the expected application of torque over time, then there must be an external load present and as such will increase power to generate the required rotational movement.

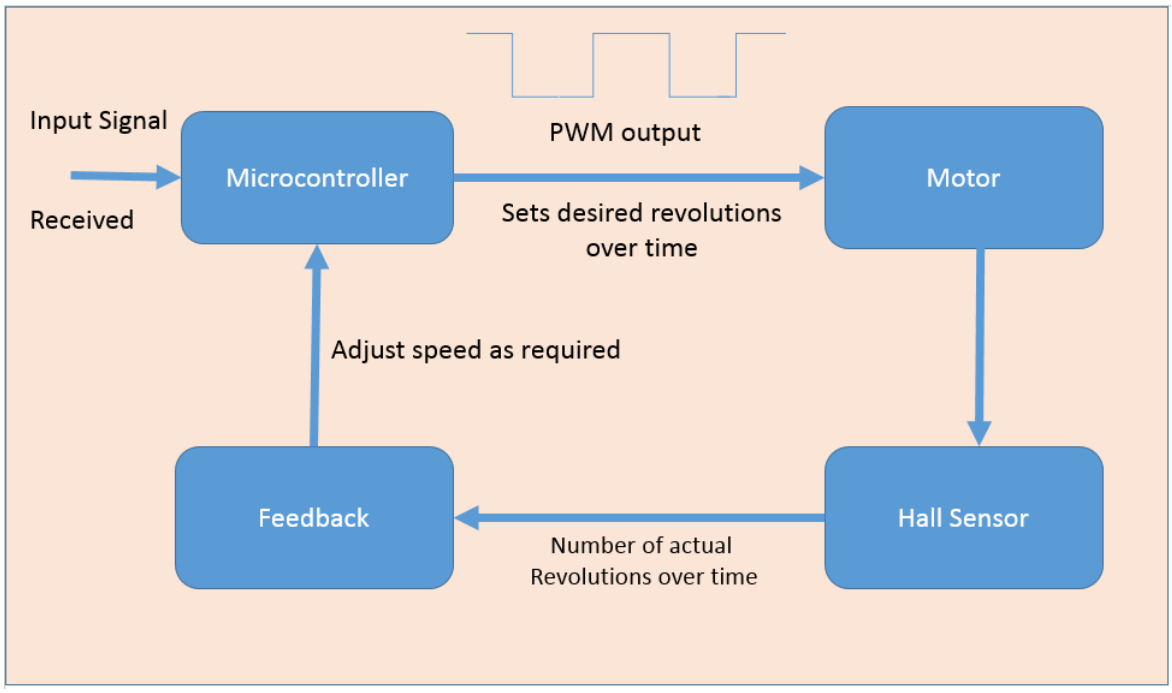

Figure 32 shows the proposed feedback loop;
> Microcontroller sets duty cycle according to measured EMG signal
> Due to no back drivability, a certain angle will directly correlate to a set number of revolutions of the wormshaft
> Hall Sensor records actual revolutions/time
> Microcontroller adjusts as necessary

4.5 PCB DESIGN

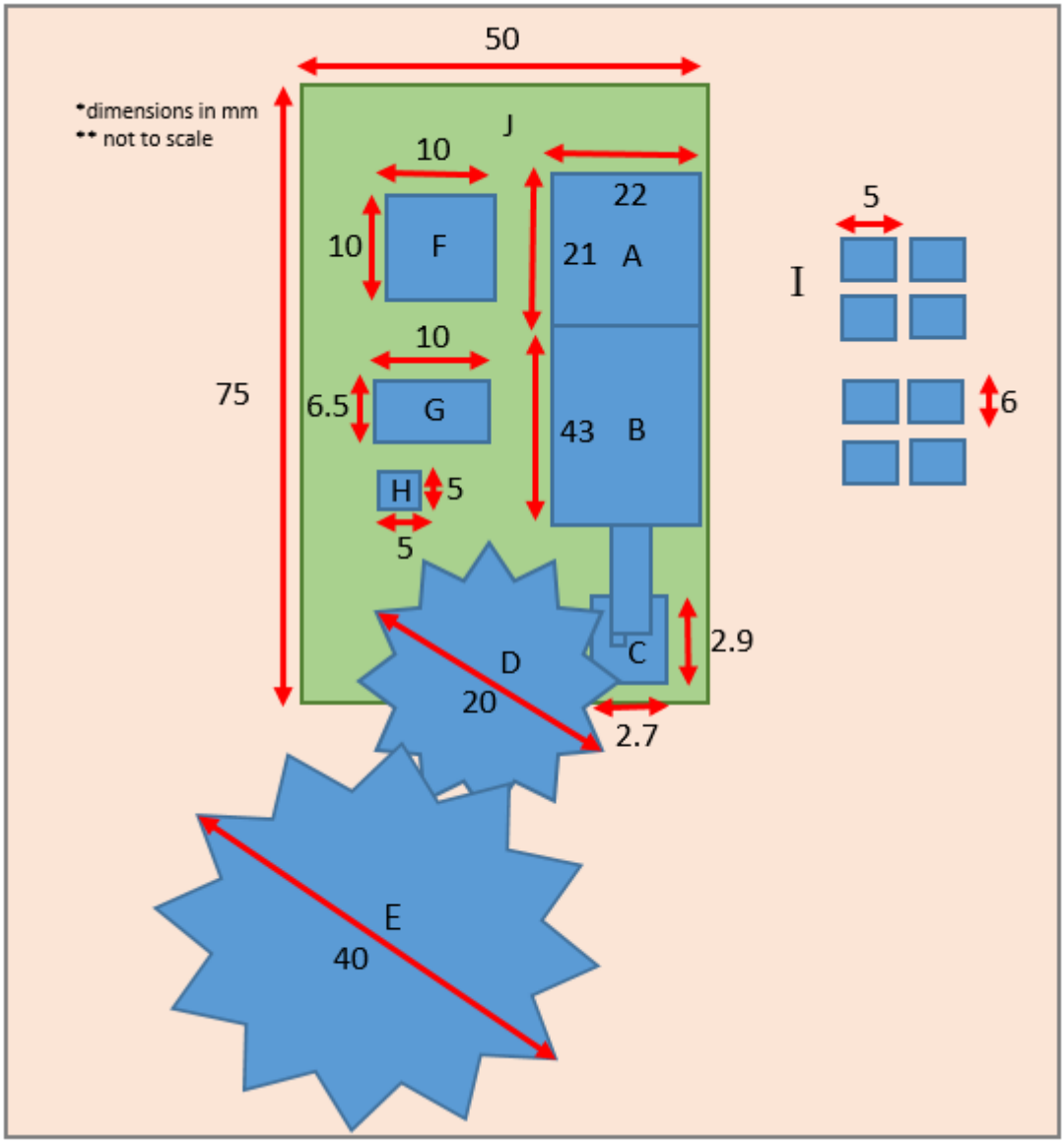

Components:-

A) Maxon A-Max Motor 12V 22Dia
B) Maxon 333:1 Planetary Gearbox
C) Hall Sensor [on PCB], Above 1x1mm Neodymium Magnet attached to Wormshaft
D) 4:1 20mm Worm Wheel
E) 2:1 40mm Spur
F) 10x10 Arduino ATMega328 Microcontroller
G) LT1167 Instrumentation Amplifier
H) Pulse Wave Modulator
I) 4x Mosfets and 4x Shottkey Diodes – L6203 H bridge
- These components will be placed on the flipside of the PCB to save space.
J) Printed Circuit Board

4-6 Pseudocode

This section will detail the microcontroller activity from sEMG electrode reading to movement and the actions that it will undertake in specific scenarios.

For a sEMG input;

The microcontroller receives this input from either the biceps or triceps from the integrated electrodes. This input will be of a certain amplitude will arrive after filtering via the instrumentation amplifier and buffer.

Based on user calibration data and myotesting, this amplitude will correlate to a specific angle of flexion and number of rotations.

> If signal originates from Bicep, apply the correct duty cycle towards flexion
> If signal originates from Triceps, apply the desired duty cycle towards extension.
> During movement, receive information based on rotations and time between 'clicks' of the hall sensor/neodymium magnet unit.
- During prototyping, these numbers [torque/rotation/time between clicks of no load] will be calculated on a per-patient basis to get the most accurate force control.
> If less rotations than expected, increase torque until expected rotation count reached and stop motor.
> If more rotations than expected, reverse direction and increase torque until expected rotation count has been reached and stop motor.

SAFETY;

As the device will be used autonomously by the user – with some mandatory check-ups to ensure progress – the device needs several features to prevent harm or damage coming due to potential motor/calibration errors.

> If upper limit (130 degrees of flexion reached) brake motor.
- This point will have to be measured in terms of number of clicks from the initial starting position. If, for example, it is 10 hall sensor 'clicks' then at click 10 the motor will cease.
> If lower limit (13 degrees of flexion reached) brake motor.
- This point will be the lower limit as set by the professional, the microcontroller must count which 'click' position it is at between 0-10. At click '0', the motor will cease.
> If signal received and duty cycle applied accordingly, if no rotations are accomplished in 3 seconds (I,e large overloading or failure of system) return to neutral angle of 20 degrees and power down.
> If two high amplitude sEMG signals received at the same time (patient is tensing), no movement [this amplitude limit will be deemed during myotesting].

4-7 Microcontroller

For the purposes of prototyping the firmware aspect of this project, the Arduino Uno board was chosen in order to speed development. Due to the multi-faceted nature of the project, ease-of-use was one of the primary concerns for the microcontroller.

The Arduino Uno board has several key aspects for which it was chosen:

- **A maximum Sample rate of 16Mhz:**
  This is fast enough to accurately make sense of nerve impulses (which are 20+Hz) and keep track of revolutions by sensor. Both of these aren't particularly memory intensive; as sEMG signals run between 20-450Hz and the maximum revolutions per minute will be 7RPM, or 14RPM with two magnets on the wormshaft for increased resolution
- **A resolution per ADC of 10 bit.**
  Resolution is important for an ADC, as it gives a clearer picture of the original signal in digital format. 10 Bits of resolution gives 1024 distinct input levels.
- **6 Analogue input pins and 14 Digital I/O pins (6 of which provide PWM input)**
  The demands of the project only require 2 analogue input pins, one for the biceps sEMG and one for the triceps sEMG signal. Additionally, only one digital I/0 input required for the Hall sensor, and one for the PWM input.
- **7-12V Power System**
  The battery pack and motor was chosen to be 12V as it can be easily accommodated by the 12V power rating of this microcontroller without use of buck convertors.
- **32Kb Memory**
  This project is not particularly memory intensive; in order to deem the torque/time/revolutions, would require knowledge of 3 or four points of data at a time.
- **Easily reprogrammed**
  For this device, the hardware requirements of the controller are not particularly demanding, however the design and implementation of the programming is imperative to the operation of the system. The Arduino Uno board, however, has a large development community and is designed to make the controller – the ATmega328 – easily programmable via a USB-based program. So this removes time constraints and restrictions that would be applied due to inexperience or lack of expertise.

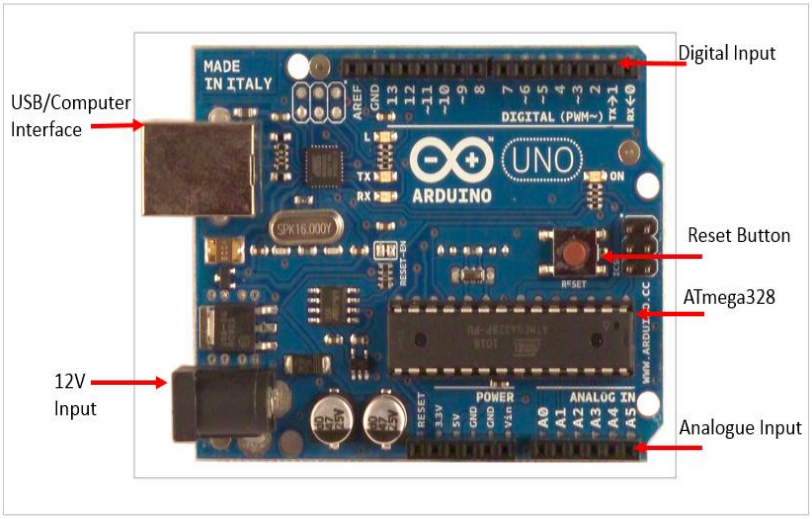

Figure 34 (left) shows the Arduino Uno board and its main components, also seen is the ATmega328. The ATmega328, after programming, would be removed and integrated onto the PCB described in section 4.5
SOURCE: Arduino Uno Datasheet

Chapter 5

Full Orthotic Design

5-1 Anthropometry of the Upper Arm

Now that the actuator has been designed and programmed, it is necessary to design the exoskeletal component of the device that will fit the arm and allow the actuator the flex and extend the elbow. As previously stated, this exoskeleton must be comfortable, safe and most importantly, adjustable. One of the self-defined design requirements was that the orthotic must be mass-producible; to accomplish this, the orthotic will therefore be designed with the goal of being applicable to 90th percentile of the population – both male and female.

According to the National bureau of size standards the following results presented represent the ranges in which the 90th percentile of males and females fit:-

----------	Male Minimum [cm]	Female Minimum [cm]	Male Maximum [cm]	Female Maximum [cm]
Bicep Circumference	33	28	43.2	35.56
Forearm Circumference [At ulnar point]	27.4	19.8	32.7	24.1
Shoulder -> Elbow Length	33.8	27	39.37	32.5
Forearm Length*	----	21.5	29.2	----
Wrist Circumference *	------	13.7	16.2	-------
Wrist Diameter **	------	4.3	5.1	-------
Elbow -> Bicep Centre of Mass ***	14.7	11.7	17.1	14.17

Table 6 shows the minimum (below 5th percentile) and maximum (90th percentile) measurements for key upper-limb sections in both males and females that will be relevant to design of the exoskeleton.

*** =Anthropometry And Biomechanics, NASA.gov, 95th percentile**

**** Calculated from Circumference measurements**

***** Calculated using Plagenhoefs data (43.6% of length from proximal end of the humerus)**

Using this data, the device must be able to conform to both the female minimum size and extend to fit the largest male whilst operating optimally at either setting. Considering the shoulder -> elbow length recorded measures from the top of the shoulder to the very bottom of the elbow; the bicep strut will not go the entire distance. Instead, it must at least cross the centre of mass, as calculated above. There is a difference of 5.4cm length between the COM female minimum and maximum, the device must be adjustable to this degree.

5.2 The Exoskeletal Design [Bicep]

Figure 35

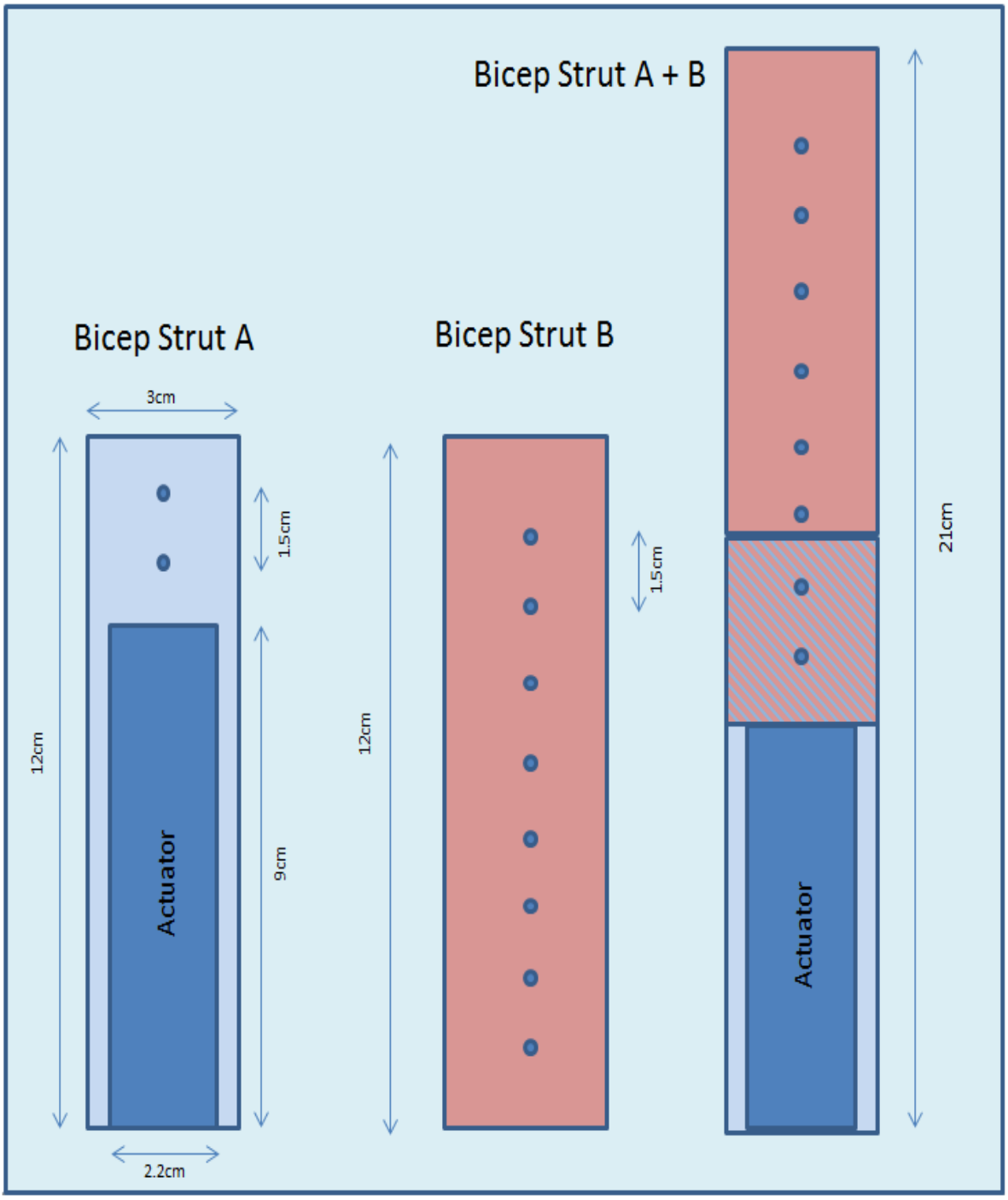

Figure 35 shows the dimensions of the two steel struts that will allow the adjustability of the orthotic. In this diagram, the actuator has been simplified to a 9x2.2cm rectangle. The struts would be adjusted to the desired length, from a minimum length of 12cm to a maximum length of 21cm and then screwed into place – satisfying the adjustment requirements. Additionally, the struts will be designed from lightweight steel and will consist of two thin plates atop one another due to time constraints. Preferably the struts would complement each other in shape to provide a stronger fit.

5.3 Exoskeletal Design [Bicep Cuff]

Figure 36

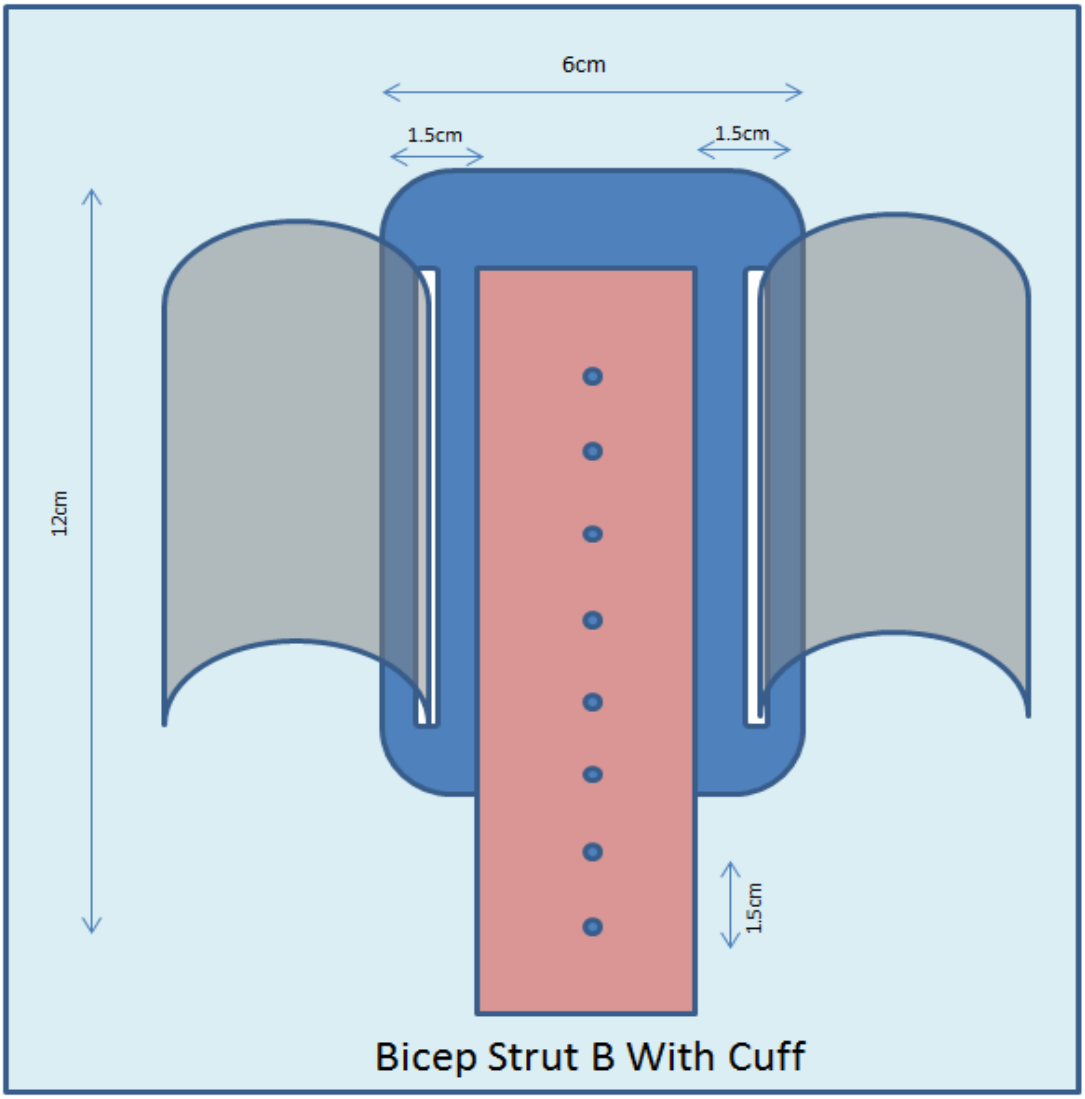

Figure 36 shows the Bicep Cuff (B) as seen in figure 35, with the proposed cuff. The blue cuff will be flat and made of a lightweight pre-preg carbon fibre, which is easy to manufacture and to in-lay the steel strut. Fed through two small gaps in its structure will be a neoprene wrap with Velcro ends to allow comfort and adjustability around the circumference of the bicep. Additionally, the carbon fibre material will have a soft backing material that is breathable for comfort and to prevent excessive sweating during use.

The width of the bicep carbon fibre cuff is 6cm; using the circumference data from section 5-1, it is possible to calculate the minimum diameter of the 5th percentile female using the equation;$\boldsymbol{Circumference = \pi * Diameter.}$ This equation gives a width of 9cm diameter; this determines that this cuff would be suitable for even the smallest adult forearm. The flat nature of the cuff, as opposed to a slight curve, is designed to prevent the curvature digging into the arm of a larger 90th percentile male bicep.

5.4 Exoskeletal Design [Forearm Struts]

Figure 37

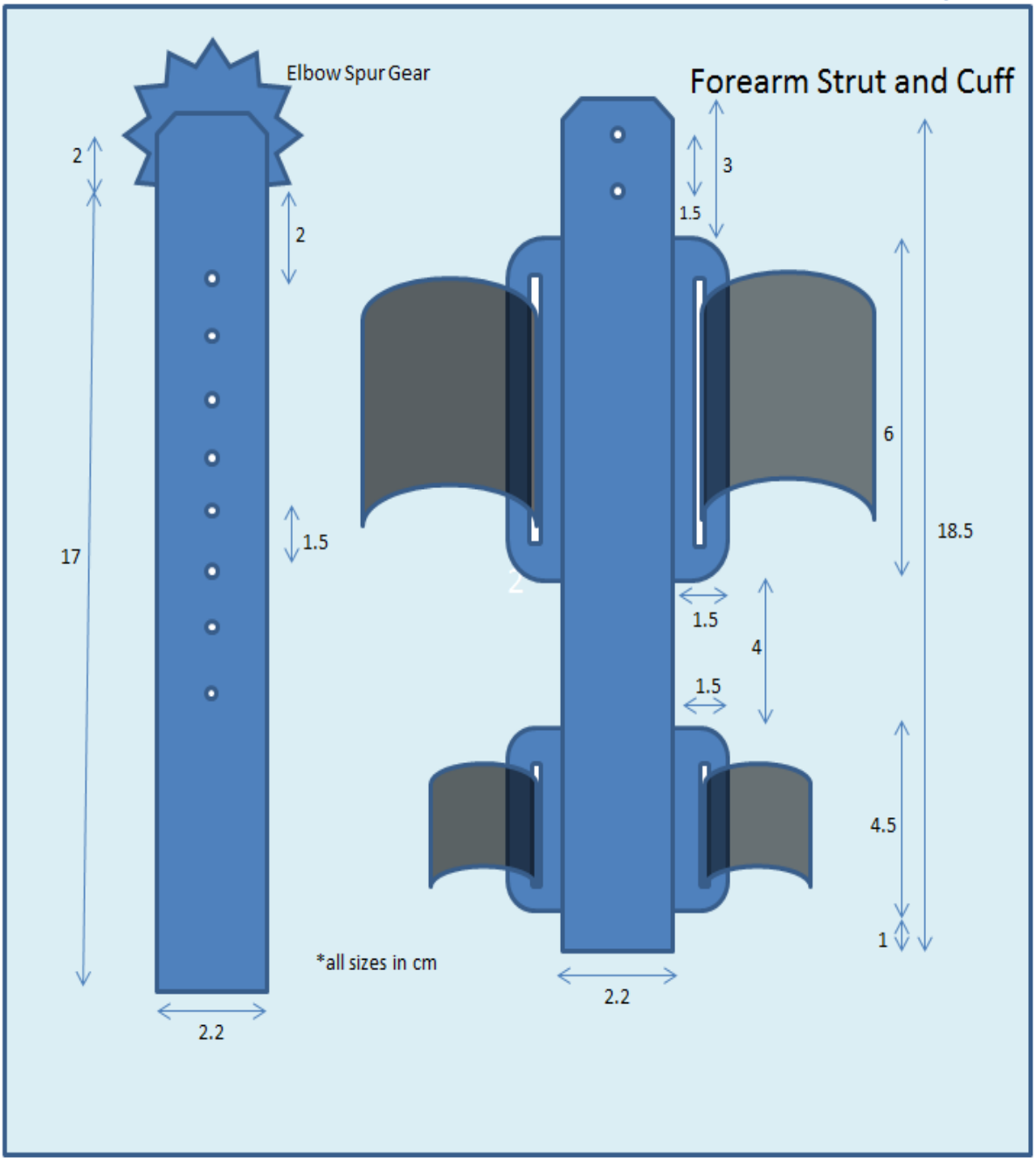

Figure 37 shows the forearm steel strut and carbon fibre cuff design. The First strut is directly attached the axle of the spur gear (shown not to scale), to allow torque to be transmitted to the forearm. The second strut has the carbon fibre cuffs with neoprene wrapping to allow a comfortable fit. Due to the natural shape of the arm, the wrist cuff will require extra padding to prevent any axial movement damaging the components in the actuator.

The total width of the struts are 2.2cm, and combined with the carbon fibre cuffs a width of 5cm; small enough to fit comfortably on the smallest percentile of females and the largest males.

The design itself has a smallest length of 19.5 cm to a maximum length of 30cm - satisfying adjustability requirements for the 5th percentile female (21.5cm) and the 90th percentile male (29.2cm). Additionally, like the bicep struts, the prototype will have simple over-laid steel struts to reduce engineering due to time constraints.

5.5 Full Proposed Design

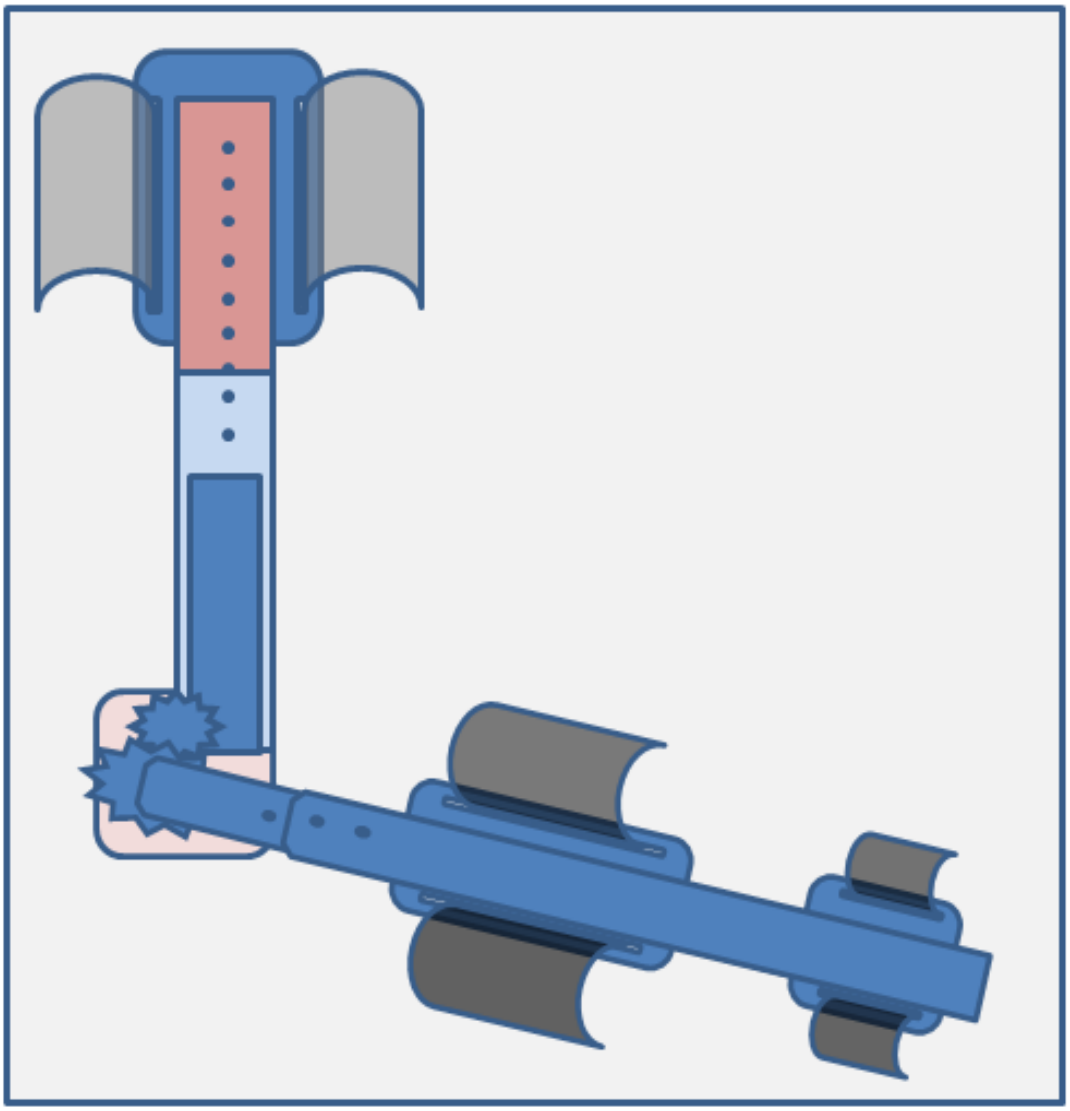

Figure 38 shows the fully designed proposed orthotic that will be built to the dimensions previously described in section 5. Seen above are bicep struts A and B with conjoined actuator as described in section 5.2 and 5.3. Additionally, the gear train consisting of the 4:1 worm wheel and 2:1 spur gear as described in section 3.13. Joined to the gear train is the forearm strut of the dimensions stated in figure 25 of section 5.4. Also seen here, though not described in the form of dimensions is a steel backplate which will house the axles to hold the worm wheel and spur gear in place.

Specifications of the full device

Total weight = <1.5Kg,
Total cost = <£200
Minimum Length (Bicep) = 12cm **Maximum Length (Bicep) = 21cm**
Minimum Length (Forearm) = 19.5cm **Maximum Length (Forearm) = 30cm**

5.6 Subluxative Fix

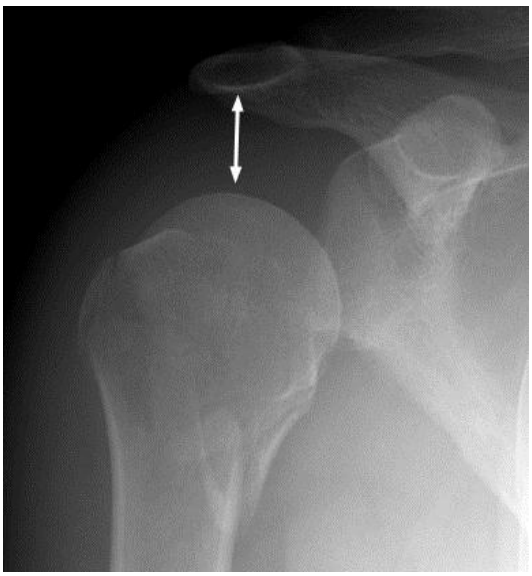

Figure 39 shows an example of subluxation, as described in section 5.6. The Humerus in this case as dropped significantly out of the glenohumeral socket, causing lack of control and sensation.
SOURCE: - Dr Jeremy Jones et al. Shoulder Dislocations – 13 case studies.

In addition to the actuated exoskeleton, one of the key issues that must be addressed – in order for the device to be a success- is subluxation. As previously mentioned, the condition of subluxation occurs in a hemiplegic arm because gravity pulls the now-unsupported humerus out of the glenohumoral socket. This leads to contraction of the internal rotators/adductors without an antagonistic muscle to prevent contracture. This often causes pain and an internal rotation of the shoulder – delaying and often preventing full rehabilitation. This, without some sort of preventative mechanism, would be compounded by the weight of the orthotic and could render the orthotic harmful, rather than rehabilitative.

There have been numerous studies on the effect of joint compression on the stability of glenohumeral joint [92]; compression of the joint essentially occurs through simulated muscle action – usually the deltoids and supraspinatus would pull the humerus in a diagonal-vertical line (see figure 40). Saha et al. found that the rotator cuff muscles act in an angle with respect to the joint surface- creating a compressive effect to 'force' the humerus into the glenohumeral joint [93]. Perry et al. compounded on this to determine that the rotator cuff muscles – made up of numerous small lever arms – generated approximately 680N of force in the average 70kg man with an arm weight of 3.5kg. Thus, with the addition of a 1.5kg orthotic, approximately 800N of force would be required to maintain stability and joint compression [94].

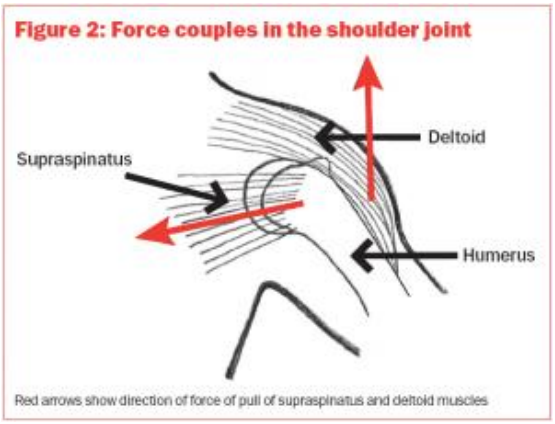

Figure 40 shows the distribution of forces due to the lever arms of the deltoid and supraspinatus muscles. The combined force leads to resultant force that is diagonally vertical.
SOURCE:- Dutton, Mark. *Orthopaedic Examination, Evaluation, and Intervention*. Second edition. The McGraw-Hill Companies, Inc, 2008. [95]

However, Warner et al. found that by using an elastomeric device to create a concave, and equally spread compressive force this can be reduced to 100-120N to stabilize in all circumstances; combined with 1.5Kg orthotic this would approximately be 200N [92].

5.6 Subluxative Fix (Cont.)

There are many forms of subluxative aids on the market currently, from shoulder straps to hemiplegic tapes and neoprene shoulders, to which there are several advantages and disadvantages. The issue with many subluxative fixes such as the hemiplegic shoulder strap (figure 42) and some Neoprene shoulders is that although they have very good positioning and proprioception, they often require custom tailoring – not suitable for our purposes. Others are hard to don by the patient themselves with their one functioning arm (hemi hook harness – Figure 42), and others not applicable for use alongside an active orthotic (such as an arm sling).

Figure 41 shows a commercially available Subluxative aid that is made of neoprene developed by Provectus Medical Ltd. This is a good example of a anti-Subluxative measure that could be used in combination with the proposed novel actuator, as it is thin enough that the bicep cuff can sit on top of it.
SOURCE: Provectus Medical Ltd. Shoulder Support Datasheet

So for this project, the sling must be able to fit the 90th percentile of patients, be comfortable and lightweight whilst also preventing subluxation. The orthotic (see right) is a commercially available orthotic that fits the requirements; however, the bicep is comprised of a neoprene polymer which is not readily adjustable. The chest size is, however, largely adjustable and the thickness is also only 3mm thick meaning that the bicep actuator could easily fit over the bicep wrap. If the time was available, it could be possible to fit a Velcro strap to the bicep to allow it to fit a wider range of patients.

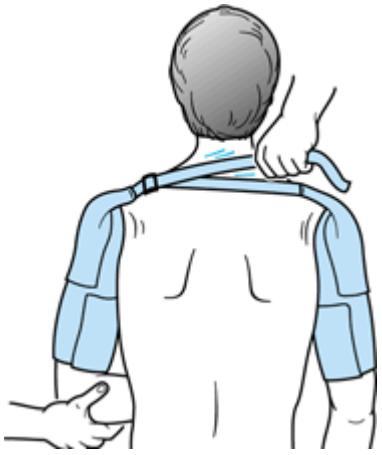

Figure 42 shows the Hemi-Hook Harness orthotic – which transfers load into the functioning shoulder.
SOURCE: The Biomet Hemi Hook Harness

Figure 43 shows a simple arm sling- cheap and effective anti-subluxation measure, but would not allow application of an active orthosis
SOURCE:- Mak-6 Shoulder Arms and Braces

Chapter 6

Discussion and Conclusions

This section will analyse whether the designed novel orthotic met the design requirements as stated in section 2-1:-

i) The mass must be low, less than 2kg to avoid disturbing function
ii) Accurate compensation for external forces
iii) Safe operation and proprioception for the patient
iv) Reliable in environments where water or grease may be present
v) Low complexity/maintenance and low engineering/construction costs
vi) Simple donning and doffing of the orthotic
vii) Must meet variable resistance targets
viii) Portability
ix) Mass Producible to 90th percentile of patients

6-1 Theoretical Analysis

Theoretically, the orthotic was designed to all specifications. However, the exoskeleton proposed lacks an outer-case which would be required to prevent debris/damage towards the internal mechanisms. This would not be particularly hard to do – given time – as it could just be a cheap, durable polypropylene housing for the actuator and gear train. Every other component is adequately lined with soft breathable material. A design for the casing has been suggested in section 6.12.3
Otherwise, the proposed design would theoretically meet all other design criteria:-

i) The mass of the orthotic is low, with a weight of <1.5Kg
ii) Neodymium magnet/Hall sensor unit compensates for external loads up to 5.5Kg.
iii) Safe operation would be possible with the aforementioned polypropylene housing; however, the ability to mould plastics was not within our capabilities. Additional safety features have also been described in section 6.12.
iv) The polypropylene housing would provide cosmesis and safety of the components in dusty/greasy environments.
v) The brushed motor may require some maintenance/checks due to internal friction, and the whole unit has a total cost of ~£200, including the actuator cost of £135.
vi) Velcro straps of the bicep and forearm cuffs allows for easy donning and doffing with the off-hand of the patient
vii) The DC motor combined with the easily programmable Arduino Uno board allows variable resistance targets to be easily met for targeted rehabilitation
viii) The battery pack, and low power requirements of the device guarantee's portability with a 20hr battery life.
ix) The adjustable length struts, easily adjustable Velcro straps and small carbon fibre panels ensure that the orthotic will fit up the 90th percentile of patients

6-1 Theoretical Analysis [Continued]

6.11- Material Selection

In any design project the goals of material selection is to minimize costs and engineering whilst maintaining the ability to accomplish the required task. For this project, the panels present on the bicep and forearm need to be able to strong enough to hold the steel struts in place whilst maintaining structural integrity. For this design, ovular gaps were cut in either side of the panels to feed through the Velcro straps (see figure 5.3) – this would weaken the integrity of any material chosen and such the material chosen must have a high tensile strength and low ductility to prevent deformation or fracture.

For these purposes, several materials which are commonly used in orthotics could be used such as steel or high strength thermoplastics like polyurethane. To maximize potential external loads and reduce the possibility of exacerbating subluxation – steel, although strong enough for the requirements, would add too much weight to the orthotic and was therefore discounted.

Instead, due to the availability of it within the NCPO, pre-preg carbon fibre was used. Pre-preg carbon fibre is carbon fibre composite which is reinforced with an epoxy resin to increase the durability of the material. This material is a low weight, high strength material that is perfect for the purposes of this project.

However, it is often expensive to source – requiring a large high-temperature autoclave unit and it requires a large amount of expertise to fabricate. In this case the equipment, material and expertise were available. Often carbon fibre orthotics will be personally cast and tailored to a patients size, but due to the mass-producible requirement of this project, the panels were designed to be flat, but small enough in diameter that this flatness would not be 'hanging off' the outer diameter of the arm of even the smallest 5^{th} percentile female.

Another viable material choice – given the manufacturing equipment – would be to use a strong thermoplastic such as polyurethane in order to reduce costs.

Bicep and Forearm Struts

Due to the expensive nature of pre preg carbon fibre, it was not possible to use carbon fibre for the full design. This could be an option if cost was not an issue; however, to reduce costs the bicep and forearm struts were made with Steel to the dimensions shown in section 5.3. Due to the lightweight nature of the actuator and carbon fibre panels, the weight of the orthotic was not hugely affected.

Upper Arm/Forearm Wrap

For the adjustable upper arm and forearm wraps, elastomeric material would be used with Velcro ends to hold in place; giving a secure and easy to don fit for users. This material is also breathable, comfortable, cheap, and easily adjustable with Velcro straps.

6.12 – Safety and Maintenance Issues

6.12.1 Brushed Motor Maintenance Issues

Due to the selection of a brushed DC motor over a brushless DC motor – chosen to minimize costs and increase the battery life – there is an added issue of maintenance. A brushless motor functions when a DC current is applied to external coils, which drive the internal rotor – producing torque. This also requires an internal controller to switch current in the motor windings – increasing complexity and costs. However, a brushed motor uses carbon brushes that rub the commutator plates – generating charges to the different commutator segments. This thus switches the polarity, and keeps the motor rotating – it is this brushing mechanism that can cause maintenance issues. The constant friction can wear down the brushes, reducing efficacy and therefore cycle life. This offers a cheaper and simpler mechanism of force control when compared to brushless motors – but also greatly increases wear and reduces lifespan [95].

As the motor will be rarely running at a torque maximum – this may or may not be an issue. The proposed orthotic would have to undergo field testing, and determine how often maintenance of the brushes are required. If the amount of maintenance outweighs the expenses of a brushless motor in addition to increasing battery size to compensate the brushless motor – then a redesign of the orthotic to accommodate the brushless motor may be better.

6.12.2 Overcharging and Overdraining

Additionally, the choice of the Lithium polymer batteries was due to the inherent low-weight to high power rating of these batteries These LiPo batteries can cause safety issues – which can be a concern as patients are expected to use the orthotic for extended periods of time without supervision. Lithium polymer batteries can be subject to overcharging and overdraining – leading to possible battery death and loss of recharge-ability or even overheating and fire. These are not acceptable risks for a medical device; as such thermal protective circuitry must be purchased or designed to protect the battery, the device and most importantly the user [96].

Some LiPo batteries come with protective circuitry installed, such as the Deben or Tracer Power brand batteries – at a very high cost. If the designer had the expertise, these high costs for protection can be circumvented by the addition of a temperature sensor, and a protection circuit such as the one seen below in figure 44. If both safety and cost are both concerns and one cannot design a protective circuit, it may instead be a better idea to use NiMH batteries – though heavier and bulkier – the batteries in this design can be carried on a waist belt to minimize obstruction.

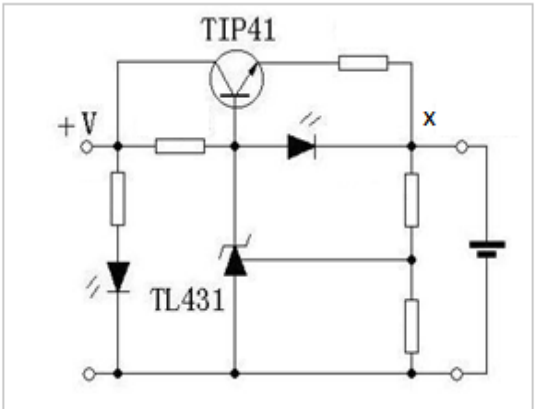

Figure 44, left, show an overcharging protection circuit; As the battery is charging, the potential at point X is increasing, and as such the TIP41 transistor is getting less forward-biased. The two TIP41 resistors would then have to be adjusted to the maximum voltage required, at which point the NPN forward biasing voltage dips below cut off range. At this point, the transistor cuts off voltage and stops charging – preventing overheating of the battery pack.

6.12.3 Overextension and Over flexion

The H Bridge described in section 4.51 has electronic braking mechanisms in place to prevent overextension and overflexion on a certain 'click count' of the neodymium magnet and hall sensor unit. However, failure of this system combined with the potential of the actuator to produce 16.2Nm could be catastrophic to the system and the user of this device.

Therefore some form of mechanical brake and secondary electrical safety feature would be beneficial to the design of the orthotic. The mechanical brake could simply be implemented into the polypropylene housing of the gear by mechanically limiting the ROM of the spur gear by rubber stops (see figure 44). Pylatiuk et al states that the average daily ROM of a person is between 0° and 165° [46], however, Murray et al. states that mechanical limits of 30° degrees towards extension and 130° degrees is where most daily tasks take place between [97] – this ROM will be chosen to have a large safety margin for the patient whilst still maintaining functionality.

The microcontroller will be programmed to recognise this mechanical stop point by initiating a category 1 stop (see description in Table 7) if torque is being produced but no rotations have occurred within 3 seconds. The compressible nature of the rubber will allow a bit of deformity during this time to prevent any possible structural damage. These rubber mechanical stops also prevent damage to the patient – but if the system has malfunctioned to the point where the motor is still producing torque and the microcontroller has not recognised the stop signal, the motor may burn out. There must, therefore, be a final safety solution in order to prevent both the user and the components should the actuator become fully miss-calibrated and is malfunctioning enough to not recognise microcontroller stop signals.

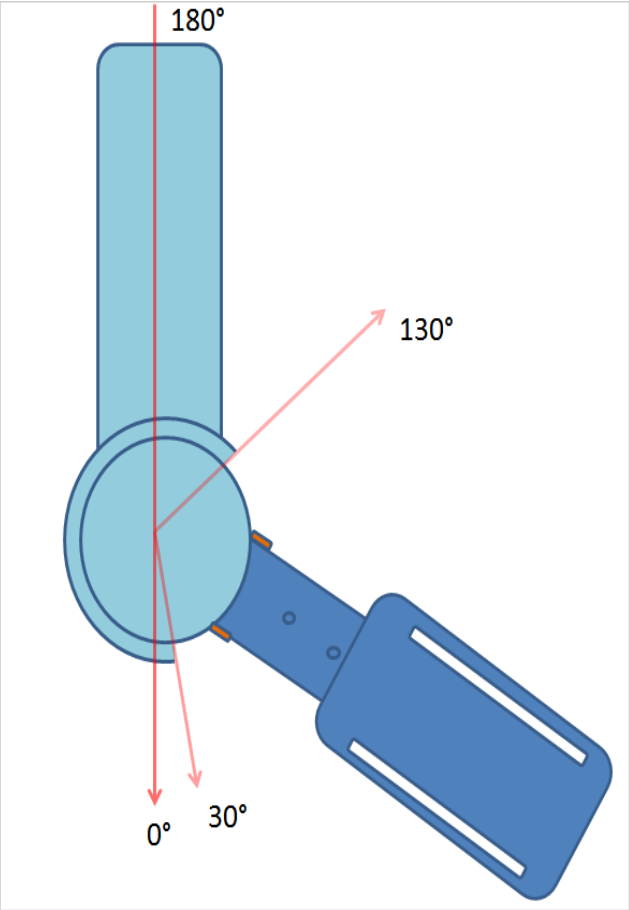

Figure 44,left, shows a potential housing design for the polypropylene; with two rubber mechanical stops either side of the spur axle to prevent extension over 13 ° and flexion over 130 °.

6.12.3 Overextension and Overflexion [Cont.]

For this reason, a secondary independent electrical safety button may be of use to entirely switch off the device before the internal components or user can be damaged. This could be done by implementing a double contact switch to the in the circuitry connecting the battery to the microcontroller, thus initiating a category 0 stop; killing and removing all power regardless of possibility of damage to components.

Table 7 - Mechanisms of Braking

Order Of Braking	Stop Mechanism*	Occurs when
1st	**H Bridge** **Normal Functional Stop**	**After set limit of Clicks**
2nd	**Compressive Mechanical Stops** **Category 2 Stop**	**Physical stop of movement**
3rd	**Microcontroller** **Category 1 stop**	**Torque is being produced in either direction, but no clicks have been 'heard'**
4th	**Emergency Double contact switch** **Category 0 stop**	**Individual chooses to shut off all power to the system immediately**

***Stop Definitions**

Normal Stop – Motor function as usual, but no more torque produced in that direction

Category 2 – Controlled stop, Power supply to components uninterrupted

Category 1 - Controlled stop, Power to actuator removed, 4 second time delay to power down.

Category 0 – Uncontrolled Stop, immediate (<200ms) shut down of power to components

6-2 Practical Analysis

Practically, due to time constraints, it was not possible to order the actuator components or electrical components in order to complete prototyping. However, the carbon fibre panels and steel exoskeleton were designed to specification, and would have likely have functioned as expected – though this cannot be stated as fact.

Considering actual construction of the exoskeleton; due to time constraints, the carbon fibre panels had to be made before the steel struts – as such, it was impossible to in-lay the steel struts into the pre-preg carbon fibre panels. This meant that it was necessary to drill and screw the steel struts onto the carbon fibre panels; this is not necessarily detrimental to the overall structure and strength, but adds extra engineering work that would not have been present if the steel could be simply in-laid into the carbon fibre panels.

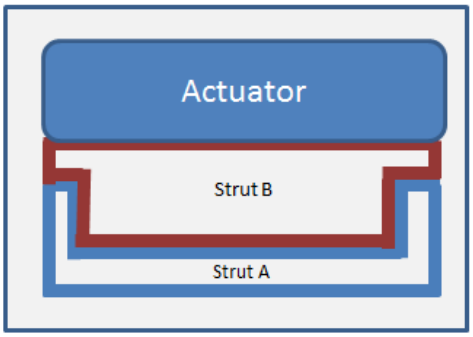

Figure 45 shows a potential theoretical complementary shape of the steel struts – shown here as an example is the bicep struts.

Additionally, the adjustable steel struts in this research were simply designed to be screwed on top of each other to reduce engineering costs and manufacture time. This is not preferable, as it means it would concentrate shear forces upon the two screws holding the struts together on the forearm and upperarm. It would be much more preferable to have complementing struts that slid into one another to form a tight fit. This would spread the stress of movement around the whole structure, rather than concentrating shear forces on the screws (see figure 45 and 46 for alternatives). This may prove to be an issue during prototyping, and the devices capability to move the arm at maximum torque without deformation and fracture would have to be adequately measured.

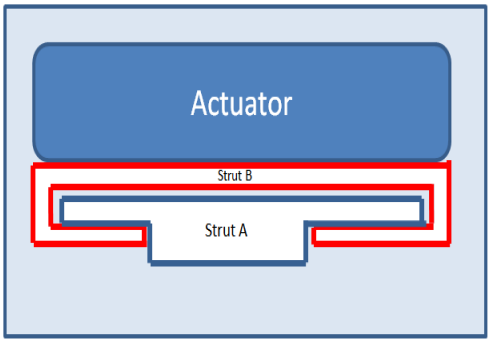

Figure 46 shows another possible configuration that would greatly increase the structural integrity of the exoskeleton.

The subluxative support, as discussed in section 5.6 also was not ordered – but would have been expected to work as stated as it is commercially available. The issues with the chosen support is that the bicep strap was not adjustable to every size – with the commercial version being marketed in a variety of sizes. If the materials and expertise was available, it may have been possible to alter the design – attaching Velcro straps around the bicep to adjust to fit the 90th percentile of patients. It is thought that it is a benefit to have the shoulder subluxative separate from the main body of the actuator – provided that the wrap is thin enough – as it makes it easier to don and doff for the patient.

6-3 Prototyping and Future Work

In order to continue the research presented in this thesis, it would be necessary to prototype the proposed unit. This should first be done separately on a breadboard to test the validity of the components and their actual output. If the actuator works as expected, this could then followed by integration onto a PCB as described in section 4.5. After construction of the actuator, a signal generator would be used to test the system against an array of low voltage (mV) 'sEMG-type' signals. This would have to be done at no load (just the exoskeleton), light load (3kg – Standard 70kg Male arm), maximum load (5.5Kg) and overload (>5.5Kg). This test would have to include the interference frequencies as would be expected as described in section 4.41 to ensure their removal and the generation of a smooth sEMG signal.

After testing the effectiveness of the signal processing and movement systems, the mechanical design would have to be prototyped – initially in terms of comfort, and how easy the device is to put on single-handedly and then the comfort after extended wear times and use. Additionally, special attention must be paid to the 4 safety stop features, with a rigorous testing of the occurrence of each possible system failure – from normal controlled stop to a category 0 stop.

If the device fails in any of these aspects, the failure will be identified and redesigned in a second prototype.

6-4 Conclusions

In reference to the design aims stated in section 2-1, the proposed novel orthotic could theoretically be called a success. The manufacturing and componentry of this project is much cheaper than the costs of current commercially-available hydraulic, pneumatic or electrical-drive orthotics. The proposed orthotic also offers a much cheaper solution to the Benitez et al. worm drive, or the MACCEPA system in terms of positional encoding and force feedback. The biggest success in this paper is the identification of the practical value of the neodymium magnet/Hall sensor unit as an easily applicable and cheap form of force control. This system is not widely used in orthotics, but could improve many systems due to its simplicity in coding, application and data requisition.

In addition, this unit would theoretically produces the same outcome as the previously mentioned drives in terms of rehabilitation, safety and power – in a relatively slim line and low mass device that is physically unobtrusive to the user. The mass and costs of the orthotic could even be further reduced by having the carbon fibre panels be replaced with a strong thermoplastic.

In conclusion, this research has produced the theory behind an orthotic that would be novel, portable, low cost, accessible and would be able meet the variable resistance targets required for successful rehabilitation. The proposed orthotic also has the potential to outperform current market orthotics in terms of external load carrying capability and portability. However, due to severe time constraints the device could not be manufactured and prototyped. As such, further work towards the development of this design may produce a marketable and effective rehabilitative orthotic.

Chapter 7

References and Appendix

7-1 REFERENCES

[1] Walsh, J., Kandamany, N., Ni Shuibhne, N., Power, H., Murphy, J. and O'Herlihy, C. (2011). Neonatal brachial plexus injury: comparison of incidence and antecedents between 2 decades. *American journal of obstetrics and gynecology*, 204(4), pp.324--1.

[2] Medscape.com, (2014). *Part 2. Physical Characteristics/Management of BPI: Characteristics of BPI*. [online] Available at: http://www.medscape.com/viewarticle/514539_2 [Accessed 11 Aug. 2014].

[3] Van Ouwerkerk, W., Van Der Sluijs, J., Nollet, F., Barkhof, F. and Slooff, A. (2000). Management of obstetric brachial plexus lesions: state of the art and future developments. *Child's Nervous System*, 16(10-11), pp.638--644.

[4] Hoeksma, A., ter Steeg, A., Dijkstra, P., Nelissen, R., Beelen, A. and De Jong, B. (2003). Shoulder contracture and osseous deformity in obstetrical brachial plexus injuries. *The Journal of Bone \& Joint Surgery*, 85(2), pp.316--322.

[5] Fiddian, N. and King, R. (1984). The winged scapula. *Clinical orthopaedics and related research*, 185, pp.228--236.

[6] Terzis, J., Vekris, M., and Soucacos, P, Brachial Plexus Root Avulsions, World Journal of Surgery, DOI: 10.1007/s00268-001-0058-8, Societe Internationale de Chirurge, 2001.

[7] Kerr, A.T. (1918) The brachial plexus of nerves in man, the variations in its formation and branches. Am. J. Anat. 23,285–395.

[8] Bergman, R.A., Thompson, S.A., and Afifi, A.K. (1988) Compendium of Human Anatomic Variation. Urban and Schwarzenberg, Baltimore

[9] Sakellariou, V., Badilas, N., Stavropoulos, N., Mazis, G., Kotoulas, H., Kyriakopoulos, S., Tagkalegkas, I. and Sofianos, I. (2014). Treatment options for brachial plexus injuries. *International Scholarly Research Notices*, 2014.

7-1 REFERENCES [Continued]

[10] Kennedy R. Suture of the brachial plexus in birth paralysis of the upper extremity. Br Med J. 1903;1:298–301.

[11] Sever JW. Obstetric paralysis: Its etiology, clinical aspects and treatment, with a report of four hundred and seventy cases. Arch Pediatr Adolesc Med. 1916;12:5417.

[12] Wyeth JA, Sharpe W. The field of neurological surgery in a general hospital. Surg Gynecol Obstet.1917;24:29–36.

[13] Vulpius O, Stoffel A. 2nd ed. Stuttgart: Enke; 1920. Orthopadische Operationslehre.

[14] Narakas A. Brachial plexus surgery. Orthop Clin North Am. 1981;12:303–23.

[15] Allieu Y, Privat JM, Bonnel F. Paralysis in root avulsion of the brachial plexus neurotization by the spinal accessory nerve. Clin Plast Surg. 1984;11:133–6

[16] Brunelli G, Brunelli F. Use of anterior nerves of cervical plexus to partially neurotize the avulsed brachial plexus. In: Brunelli G, editor. Textbook of Microsurgery.

[17] Hugue Ouellette (2008). *Orthopedics Made Ridiculously Simple (Medmaster Ridiculously Simple) (Medmaster Ridiculously Simple)*. MedMaster Inc. ISBN 0-940780-86-0.

[18] C. Oberlin, D. Beal, S. Leechavengvongs, A. Salon, M. C. Dauge, and J. J. Sarcy, "Nerve transfer to biceps muscle using a part of ulnar nerve for C5-C6 avulsion of the brachial plexus: anatomical study and report of four cases," Journal of Hand Surgery A, vol. 19, no. 2, pp. 232–237, 1994.

[19] S. Leechavengvongs, K. Witoonchart, C. Uerpairojkit, P. Thuvasethakul, and W. Ketmalasiri, "Nerve transfer to biceps muscle using a part of the ulnar nerve in brachial plexus injury (upper arm type): a report of 32 cases," Journal of Hand Surgery A, vol. 23, no. 4, pp. 711–716, 1998.

7-1 REFERENCES

[20] A. Sungpet, C. Suphachatwong, V. Kawinwonggowit, and A. Patradul, "Transfer of a single fascicle from the ulnar nerve to the biceps muscle after avulsions of upper roots of the brachial plexus," Journal of Hand Surgery B, vol. 25, no. 4, pp. 325–328, 2000.

[21] P. Songcharoen, S. Wongtrakul, B. Mahaisavariya, and R. J. Spinner, "Hemi-contralateral C7 transfer to median nerve in the treatment of root avulsion brachial plexus injury," Journal of Hand Surgery A, vol. 26, no. 6, pp. 1058–1064, 2001.

[22] Zsoldos, C., Basamania, C. and Bal, G. (2013). Shoulder fusion after a self-inflicted gunshot wound An injury pattern and treatment option. *Bone \& Joint Journal*, 95(6), pp.820--824.

[23] E. Rouholamin, J. R. Wootton, and A. M. Jamieson, "Arthrodesis of the shoulder following brachial plexus injury," Injury, vol. 22, no. 4, pp. 271–274, 1991.

[24] Wong, E., Kwan, M., Loh, W. and Ahmad, T. (2005). Shoulder arthrodesis in brachial plexus injuries--a review of six cases. *The Medical journal of Malaysia*, 60, pp.72--77.

[25] Atlan, F., Durand, S., Fox, M., Levy, P., Belkheyar, Z. and Oberlin, C. (2012). Functional outcome of glenohumeral fusion in brachial plexus palsy: a report of 54 cases. *The Journal of hand surgery*, 37(4), pp.683--688.

[26] RORABECK, C. (1980). The management of the flail upper extremity in brachial plexus injuries. *Journal of Trauma-Injury, Infection, and Critical Care*, 20(6), pp.491--493.

[27] Guettler, J. and Basamania, C. (2005). Muscle transfers involving the shoulder. *Journal of surgical orthopaedic advances*, 15(1), pp.27--37.

[28] Elhassan, B., Bishop, A., Shin, A. and Spinner, R. (2010). Shoulder tendon transfer options for adult patients with brachial plexus injury. *The Journal of hand surgery*, 35(7), pp.1211--1219.

7-1 REFERENCES

[29] Beauchamp, M., Beaton, D., Barnhill, T., Mackay, M. and Richards, R. (1998). Functional outcome after the L'Episcopo procedure. *Journal of Shoulder and Elbow Surgery*, 7(2), pp.90--96.

[30] R. R. . Richards, "Operative treatment for irreparable lesions of the brachial plexus," in Operative Nerve Repair and Reconstruction, R. H. Gelberman, Ed., pp. 1303–1327, J. B. Lippincott & Company, Philadelphia, Pa, USA, 1991.

[31] Y. Akasaka, T. Hara, and M. Takahashi, "Free muscle transplantation combined with intercostal nerve crossing for reconstruction of elbow flexion and wrist extension in brachial plexus injuries,"Microsurgery, vol. 12, no. 5, pp. 346–351, 1991.

[33] Birch R. Brachial plexus injuries. Instructional Course Lecture. J Bone Joint Surg [Br] 1997;78-B:986-92.

[34] Krakauer JD, Wood MB. Adult injuries and salvage. In: Peimer CA,ed. Surgery of the hand and upper extremity. New York: McGraw-Hill Co, 1995:1411-42

[35] Doi, K., Hattori, Y., Kuwata, N., Soo-Heong, T., Kawakami, F., Otsuka, K. and Watanabe, M. (1998). Free muscle transfer can restore hand function after injuries of the lower brachial plexus. *Journal of Bone \& Joint Surgery, British Volume*, 80(1), pp.117--120.

[36] Miniaci, A. and MacLeod, M. (1999). Transfer of the Latissimus Dorsi Muscle After Failed Repair of a Massive Tear of the Rotator Cuff. A two to five-year Review*. *The Journal of Bone \& Joint Surgery*, 81(8), pp.1120--7.

[37] Belter, J., Segil, J., Dollar, A. and Weir, R. (2013). Mechanical design and performance specifications of anthropomorphic prosthetic hands: A review. *J Rehabil Res Dev*, 50(5), pp.599--618.

[38] Wynn Parry CB: The management of injuries to the brachial plexus. *Proc R Soc Med*1974; 67:488-490.

[39] Bunch WH. Introduction to orthotics. In: American Academy of Orthopaedic Surgeons. atlas of orthotics Biomechanical Principles and Application, 2nd Ed. St. Louis: C. V. Mosby Company; 1985;3.

[40] Sharrard WJW. Muscle recovery in poliomyelitis. Journal of Bone and Joint Surgery (American). 1955;37B:63.

7-1 REFERENCES

[41] Fyfe N C M, McClemont E J W, Panton L E. *et al* Assistive technology: mobility aids, environmental control systems, and communication aids. In: Greenwood RJ, Barnes MP, McMillan TM, Ward CD, eds. Handbook of neurological rehabilitation, 2nd edn. Hove: Psychology Press, 2003. 725

[42] A survey on robotic devices for upper limb rehabilitation
Paweł Maciejasz123, Jörg Eschweiler4*, Kurt Gerlach-Hahn5, Arne Jansen-Troy4 andSteffen Leonhardt

[43] Galv'an, A. (2010). Neural plasticity of development and learning. *Human brain mapping*, 31(6), pp.879--890.

[44] Robinson C: Brachial plexus lesions Part 1: Management. *Br J Occup Ther* 1986; 49:147-150

[45] VukoBrahtovic, M. (2008). Active exoskeletal systems and beginning of the development of humanoid robotics. *Monograph of Academy of Nonlinear Science*, 2(2), pp.329-348.

[46] C. Pylatiuk, A. Kargov, I. Gaiser, T. Werner, S. Schulz, and G. Bretthauer, "Design of a flexible fluidic actuation system for a hybrid elbow orthosis," in Proceedings of the IEEE International Conference on Rehabilitation Robotics (ICORR '09), pp. 167–171, June 2009.

[47] Wiegand, R., Schmitz, B., Pylatiuk, C. and Schulz, S. (2011). Mechanical Performance of Actuators in an Active Orthosis for the Upper Extremities. *Journal of Robotics*, 2011.

[48] Daerden, F. and Lefeber, D. (2002). Pneumatic artificial muscles: actuators for robotics and automation. *European journal of mechanical and environmental engineering*, 47(1), pp.11--21.

[49] Eskiizmirliler, S., Forestier, N., Tondu, B. and Darlot, C. (2002). A model of the cerebellar pathways applied to the control of a single-joint robot arm actuated by McKibben artificial muscles. *Biological cybernetics*, 86(5), pp.379--394.

[50] Th. Beullens, "Hydraulic or Pneumatic Drive Device", US Patent No. 4 841 845, 1989.

7-1 REFERENCES

[51] F. Daerden and D. Lefeber, "The concept and design of pleated pneumatic artificial muscles", International Journal of Fluid Power, vol. 2, no. 3, pp. 41–50, 2001.

[52] J. Smrček, J. N. Marcinčin and J. Niznik, "The Under Pressure Artificial Muscle UPAM—New actuator in biorobotics", 5th International Symposium on Measurement and Control in Robotics, pp. 199–203, Slovak Republic, 1995.

[53] A. H. Morin, "Elastic diaphragm", US Patent No. 2 642 091, 1953.

[54] M. Kukolj, "Axially contractible actuator", US Patent No. 4 733 603, 1988.

[55] H. A. Baldwin, "Realizable models of muscle function", Proceedings of the First Rock Biomechanics Symposium, pp. 139–148, New York, 1969.

[56] H. M. Paynter, "Hyperboloid of revolution fluid-driven tension actuators and methods of making", US Patent No. 4 721 030, 1988.

[57] Schiele, A., Letier, P., Van Der Linde, R. and Van Der Helm, F. (2006). Bowden cable actuator for force-feedback exoskeletons. pp.3599--3604.

[58] Nef, T., Mihelj, M. and Riener, R. (2007). ARMin: a robot for patient-cooperative arm therapy. *Medical \& biological engineering \& computing*, 45(9), pp.887--900.

[59] J. Stein, K. Narendran, J. McBean, K. Krebs, and R. Hughes, "Electromyography-controlled exoskeletal upper-limb-powered orthosis for exercise training after stroke," American Journal of Physical Medicine and Rehabilitation, vol. 86, no. 4, pp. 255–261, 2007.

[60] S. J. Housman, V. Le, T. Rahman, R. J. Sanchez Jr., and D. J. Remkensrneyer, "Arm-training with T-WREX after chronic stroke: preliminary results of a randomized controlled trial," in Proceedings of the IEEE 10th International Conference on Rehabilitation Robotics (ICORR '07), pp. 562–568, Noordwijk, Netherlands, June 2007.

[61] B. Schmitz, R. Wiegand, Ch. Pylatiuk, R. Rupp, and St. Schulz, "Erste erfahrungen mit dem orthojacket,"Orthopädie-Technik, vol. 4, no. 11, pp. 256–261, 2011.

7-1 REFERENCES

[62] Kuiken, T., Dumanian, G., Lipschutz, R., Miller, L. and Stubblefield, K. (2004). The use of targeted muscle reinnervation for improved myoelectric prosthesis control in a bilateral shoulder disarticulation amputee. *Prosthetics and Orthotics International*, 28(3), pp.245--253.

[63] Tsagarakis, N. and Caldwell, N. (2007). A Compliant exoskeleton for multi-planar upper limb physiotherapy and training. *Advanced Robotics, Invited Paper,(submitted)*.

[64] Vanderborght, B., Van Ham, R., Lefeber, D., Sugar, T. and Hollander, K. (2009). Comparison of mechanical design and energy consumption of adaptable, passive-compliant actuators. *The International Journal of Robotics Research*, 28(1), pp.90--103.

[65] D. G. Caldwell, G. A. Medrano-Cerda and M. J. Goodwin, "Control of Pneumatic Muscle Actuators", IEEE Control Systems Magazine, vol. 15, number 1, pp. 40–48, 1995.

[66] Cherelle, P., Grosu, V., Beyl, P., Mathys, A., Van Ham, R., Van Damme, M., Vanderborght, B. and Lefeber, D. (2010). The MACCEPA actuation system as torque actuator in the gait rehabilitation robot ALTACRO. pp.27--32.

[67] Van Ham, R., Van Damme, M., Vanderborght, B., Verrelst, B. and Lefeber, D. (2006). Maccepa: The mechanically adjustable compliance and controllable equilibrium position actuator. pp.196--203.

[68] Kostuik, J.P. (1980) Amputation Surgery and Rehabilitation (The Toronto Experience). Churchill Livingstone, New York.

[69] Jardim, B. and Siqueira, A. (2014). Development and analysis of series elastic actuators for impedance control of an active ankle--foot orthosis. *Journal of the Brazilian Society of Mechanical Sciences and Engineering*, 36(3), pp.501--510.

[70] Matteo, B. (1997). The Design of an Elastic Element for a Modular Series Elastic Actuator.

7-1 REFERENCES

[71] Carpino, G., Accoto, D., Sergi, F., Tagliamonte, N. and Guglielmelli, E. (2012). A novel compact torsional spring for series elastic actuators for assistive wearable robots. *Journal of Mechanical Design*, 134(12), p.121002.

[72] Kong, K., Bae, J. and Tomizuka, M. (2012). A compact rotary series elastic actuator for human assistive systems. *Mechatronics, IEEE/ASME Transactions on*, 17(2), pp.288--297.

[73] Eshraghi, A., Osman, N., Gholizadeh, H., Ahmadian, J., Rahmati, B. and Abas, W. (2013). Development and evaluation of new coupling system for lower limb prostheses with acoustic alarm system. *Scientific reports*, 3.

[74] C. Pylatiuk, S. Schulz, H. Vaassen, M. Reischl: PreliminaryEvaluation for a Functional Support of the Elbow and Shoulder Joint.Proceedings of the 13th Annual Conference of the InternationalFunctional Electrical Stimulation Society (IFESS `08), Sept. 21-25, 2008, Freiburg, Germany. Biomedical Technology 53:77-79, 2008.

[75] De Luca, C., Le Fever, R. and Stulen, F. (1979). Pasteless electrode for clinical use. *Medical and biological engineering and computing*, 17(3), pp.387--390.

[76] Buschbacher, R., Weir, S., Bentley, J. and Cottrell, E. (2009). Normal motor nerve conduction studies using surface electrode recording from the supraspinatus, infraspinatus, deltoid, and biceps. *PM\&R*, 1(2), pp.101—106

[77] Young, A., Redmond, M., Hemler, D. and Belandres, P. (1990). Radial motor nerve conduction studies. *Archives of physical medicine and rehabilitation*, 71(6), pp.399--402.

[78] Feinberg, J., Radecki, J., Wolfe, S., Strauss, H. and Mintz, D. (2008). Brachial plexopathy/nerve root avulsion in a football player: the role of electrodiagnostics. *HSS Journal*, 4(1), pp.87--95.

[79] myotesting 3-4 weeks

[80] Mansukhani, K. (2013). Electrodiagnosis in traumatic brachial plexus injury. *Annals of Indian Academy of Neurology*, 16(1), p.19.

[81] Wee, A. (2005). Correlation between the biceps brachii muscle bulk and the size of its evoked compound muscle action potential. *Electromyography and clinical neurophysiology*, 46(2), pp.79--82.

7-1 REFERENCES

[82] Ahamed, N., Sundaraj, K., Ahmad, R., Rahman, M. and Islam, M. (2012). Analysis of right arm biceps brachii muscle activity with varying the electrode placement on three male age groups during isometric contractions using a wireless EMG sensor. *Procedia Engineering*, 41, pp.61--67.

[83] Greenberg, S. and Amato, A. (2004). *EMG pearls*. 1st ed. Philadelphia: Hanley & Belfus.

[84] Huigen, E. (2000). Noise in biopotential recording using surface electrodes.

[85] Oster, G. and Jaffe, J. (1980). Low frequency sounds from sustained contraction of human skeletal muscle. *Biophysical journal*, 30(1), pp.119--127.

[86] Trenado, C., Mikuli\'c, A., Manjarrez, E., Mendez-Balbuena, I., Schulte-M\"onting, J., Huethe, F., Hepp-Reymond, M. and Kristeva, R. (2014). Broad-band Gaussian noise is most effective in improving motor performance and is most pleasant. *Frontiers in human neuroscience*, 8.

[87] McAuley, J., Rothwell, J. and Marsden, C. (1997). Frequency peaks of tremor, muscle vibration and electromyographic activity at 10 Hz, 20 Hz and 40 Hz during human finger muscle contraction may reflect rhythmicities of central neural firing. *Experimental Brain Research*, 114(3), pp.525--541.

[88] Merletti, R. and Di Torino, P. (1999). Standards for reporting EMG data. *J Electromyogr Kinesiol*, 9(1), pp.3--4.

[89] De Luca, C., Donald Gilmore, L., Kuznetsov, M. and Roy, S. (2010). Filtering the surface EMG signal: Movement artifact and baseline noise contamination. *Journal of biomechanics*, 43(8), pp.1573--1579.

[90] van Boxtel, A., Boelhouwer, A.J.W., Bos, A.R., 1998. Optimal EMG signal bandwidth and interelectrode distance for the recording of acoustic, electrocutaneous, and photic blink reflexes. Psychophysiology 35, 690–697.

[91] Hewson, D., Hogrel, J., Langeron, Y. and Duch\^ene, J. (2003). Evolution in impedance at the electrode-skin interface of two types of surface EMG electrodes during long-term recordings. *Journal of Electromyography and Kinesiology*, 13(3), pp.273--279.

7-1 REFERENCES

[92] Warner, J., Bowen, M., Deng, X., Torzilli, P. and Warren, R. (1999). Effect of joint compression on inferior stability of the glenohumeral joint. *Journal of Shoulder and Elbow Surgery*, 8(1), pp.31--36.

[93] Saha, A. (1971). Dynamic stability of the glenohumeral joint. *Acta Orthopaedica*, 42(6), pp.491--505.

[94] Perry, J. (1983). Anatomy and biomechanics of the shoulder in throwing, swimming, gymnastics, and tennis. *Clinics in sports medicine*, 2(2), pp.247--270.

[95] Gamazo-Real, J., V\'azquez-S\'anchez, E. and G\'omez-Gil, J. (2010). Position and speed control of brushless DC motors using sensorless techniques and application trends. *Sensors*, 10(7), pp.6901--6947.

[96] Wang, B., Richardson, T. and Chen, G. (2013). Stable and high-rate overcharge protection for rechargeable lithium batteries. *Physical Chemistry Chemical Physics*, 15(18), pp.6849--6855.

[97] Dutton, Mark. *Orthopaedic Examination, Evaluation, and Intervention*. Second edition. The McGraw-Hill Companies, Inc, 2008.

APPENDIX

Subsection of Plexus	Nerve	Root Vertebrae	Innervated Muscles
Root	Dorsal Scapular	C4/C5	Rhomboid Muscles Levator Scapulae
Root	Long Thoracic Nerve	C5/C6/C7	Serratus Anterior
Root	Phrenic Nerve	C5	Diaphragm
Upper Trunk	Subclavicle Nerve	C5/C6	Subclavius
Medial Cord	Medial Pectoral	C8/T1	Pectoralis Major
Medial Cord	Median Nerve	C8/T1	-
Medial Cord	Medial Brachial Cutaneous Nerve (	C8/T1	Upper arm Skin
Medial Cord	Medial Antebrachium Cutaeneous Nerve	C8/T1	Forearm Skin
Medial Cord	Ulnar Nerve	C8/T1	Hand Skin Fingers
Lateral Cord	Musculocutaeneous	C5/C6/C7	Coracobrachialis, biceps brachii, brachialis.
Lateral Cord	Lateral Pectoral	C5/C6/C7	Pectoralis Major/Minor
Posterior Cord	Upper Subscapular	C5/C6	Subscapularis
Posterior Cord	Thoracodorsal	C6/C7/C8	Latissimus Dorsi
Posterior Cord	Lower Subscapular	C5/C6	Lower Scapular Teres Major
Posterior Cord	Axilliary Nerve	C5/C6	Deltoids Teres Minor
Posterior Cord	Radial Nerve	C5/C6/C7/C8/T1	Triceps Brachii Supinator Forearm Extensor Brachioradialis

The above table, referenced in section 1-2, shows the varying cords and the nerves originate from them. Also shown is the root vertebrae and the muscles which the nerves innervate. This table is to give knowledge on all the particular nerves of the brachial plexus, and allo it to trace how different nerve avulsions can lead to a series of different symptoms.

APPENDIX (Cont.)

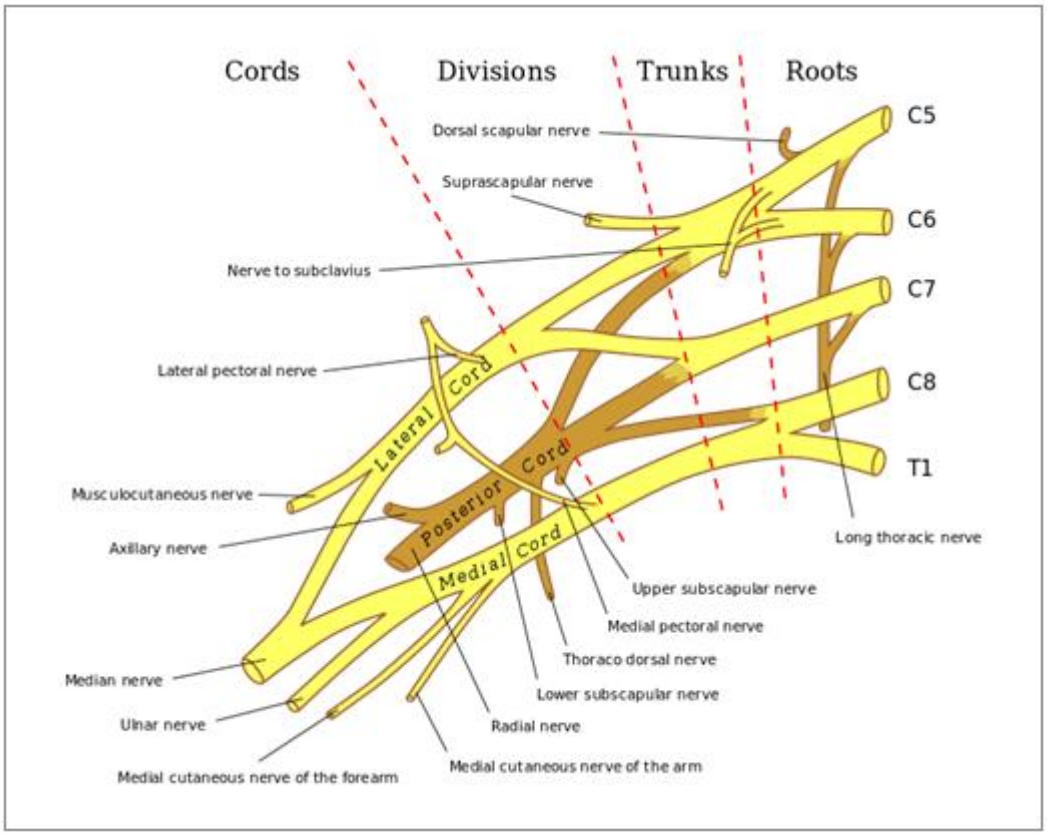

The above diagram, mentioned in section 1-2, is an in-depth view of the structure of the brachial plexus. This figure, combined with the above table allows greater understanding of the nerves and how they lead to the muscle that they innervate.